

**EXPERIMENTAL INVESTIGATION OF AIRCRAFT
WING FLUTTER CONSIDERING AERODYNAMICS
PARAMETERS TO ADDRESS WING EFFICIENCY A
COMPARATIVE TESTING**

Thesis Submitted for the Award of the Degree of

DOCTOR OF PHILOSOPHY
in
(Aerospace Engineering)

By
R Sabari Vihar
(41900444)

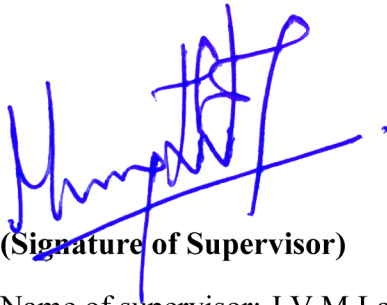
Supervised By
J V M Lal Jeyan
(22724)



LOVELY PROFESSIONAL UNIVERSITY
PUNJAB
2024

CERTIFICATE

This is to certify that the work reported in the Ph. D. thesis entitled “Experimental investigation of aircraft wing flutter considering aerodynamics parameters to address wing efficiency a comparative testing” submitted in fulfilment of the requirement for the reward of degree of **Doctor of Philosophy (Ph.D.)** in the Aerospace engineering/ School of Mechanical engineering, is a research work carried out by R Sabari Vihar, 41900444, is bonafide record of his/her original work carried out under my supervision and that no part of thesis has been submitted for any other degree, diploma or equivalent course.

A handwritten signature in blue ink, appearing to be 'J V M Lal Jeyan', written over a horizontal line.

(Signature of Supervisor)

Name of supervisor: J V M Lal Jeyan

Designation: Professor

Department/school: Aerospace engineering/ School of Mechanical engineering

University: Lovely Professional University

DECLARATION

I, hereby declared that the presented work in the thesis entitled “Experimental investigation of aircraft wing flutter considering aerodynamics parameters to address wing efficiency a comparative testing” in fulfilment of degree of **Doctor of Philosophy (Ph. D.)** is the outcome of research work carried out by me under the supervision of J V M Lal Jeyan, working as Professor, in the Aerospace engineering/ School of Mechanical engineering of Lovely Professional University, Punjab, India. In keeping with general practice of reporting scientific observations, due acknowledgements have been made whenever work described here has been based on findings of other investigator. This work has not been submitted in part or full to any other University or Institute for the award of any degree.



(Signature of Supervisor)

Name of the scholar: R Sabari Vihar

Registration No.: 41900444

Department/school: Aerospace engineering/ School of Mechanical engineering

Lovely Professional University,

Punjab, India

ABSTRACT

This study concentrates on investigating the effect of camber on the flutter behaviour of the wing fabricated from NACA five-digit airfoil. Flutter is an undesired phenomenon that occurs due to the interaction of fluid that causes aerodynamic forces with the elastic and inertial forces of structures. As the fluid interacts with the solid, the solid body starts to vibrate and as the fluid velocity is further increased, the vibrations in the solid body starts to increase, when the vibrations induced by the fluid forces overwhelm the natural frequencies of the body the structure starts to vibrate uncontrollably and will lead to catastrophic failure of the structure. When structures like aircraft wing are studied the body will start to vibrate in pitch, movement in direction of angle of attack and plunge in the direction of bending will be seen, flutter is the phenomenon that leads to vibration of wing in both pitch and plunge simultaneously and uncontrollably after certain frequencies. To avoid and delay or suppress the flutter, the primary solution is to increase the strength of the structure that in turn again will increase the weight of the structure, which is the most undesired effect especially in the era of slender wing structures. To ensure the stability of the structure without adding any equipment that in turn again will add to its weight, aerodynamics of the structure was selected to concentrate in this project, for which the camber, which is one of the crucial parameters that help in the generation of lift was selected and the location of the maximum camber of the wing was concentrated upon. The objectives behind this work is to design and analyse the flutter behaviour of different selected wing plan forms computationally, analyse the effect of camber on the flutter characteristics of different selected wing plan forms, study the flutter characteristics of selected wing plan forms analytically over prototypes and to investigate the possibility of delay or suppressing the flutter by varying the nomenclature of the wing. Wing sections with different airfoil sections by varying the location of maximum camber are fabricated by keeping all the other dimensions like wing span, chord length, etc. same across all the wing models and experiments were conducted in wind tunnel. Firstly, computational analysis was conducted on 2D wing sections for understanding the flutter behaviour with help of pitch and plunge movements of the airfoil. The experimental analysis was conducted on different airfoil sections by selecting the airfoil sections in such a way

that the location of maximum camber is varied. To conduct the experiment, accelerometers were attached to the leading edge and trailing edge of the wing, these accelerometers were connected to arduino board and were in turn connected to laptop to record values of change in acceleration with respect to time as the air inlet velocity is changed and also to observe the change in acceleration vs time graphs. The obtained results are again fast Fourier transformed to obtain the frequency of vibration. To investigate the possibility to suppress flutter of wing by varying the location of maximum camber, the variation of c_l with respect to time was studied computationally and variation of acceleration with time, frequency of vibration, the amplitude of vibration was studied and analysed. Four airfoils 21012, 22012, 23012 and 24012 were analysed, as the second digit in the NACA five digit represents the location of maximum camber in terms of chord length, the results will help us understand the effect of camber on the flutter behaviour. Based on the computational results it was concluded that it is clearly evident that the instability in pitching motion of the airfoil was more as the position of maximum camber moves closer to the centre of flexural axis on the airfoil. When the plunging motion was observed for the variation of coefficient of lift, there was an unsteady and irregular variation observed in the values of coefficient of lift this could be seen in the C_l vs time plot of the 21012 airfoil, for this airfoil the location of maximum camber is far than compared to that of the other airfoils which are 22012, 23012 and 24012 as there can be no much fluctuations to be seen in the graph of 21012 compared to the rest. Experimental results that were concluded based on the air inlet velocity at which flutter is induced and on the intensity of the flutter at specific air speeds, it can be concluded from the acceleration vs time graphs that the flutter is induced at early airspeeds when the location of maximum camber is closer to the flexural axis, which is fixed at forty percent of the wing chord. Flutter seems to induce at lower air velocities and based on the closeness of the crests in the acceleration versus time graphs, it can be clearly understood that the flutter is more rigorous in the same case. Both the computational and experimental results agree to the point that flutter is induced at early airspeeds when the location of maximum camber is closer to the flexural axis. Based on the results it can be concluded that, location of maximum camber definitely has its part to play in the flutter behaviour of the wing and based on which it can be said that the camber can also contribute to the flutter.

List of Tables

Table 1: Implicit stiffness and inertia characteristics	28
---	----

List of Figures:

Figure 1 Collars triangle	2
Figure 2: Aero foil structure	29
Figure 3 Wing installed with Arduino and accelerometers.	29
Figure 4. CAD file.	30
Figure 5. Ribs laser cutting.	31
Figure 6. Ribs and spars after laser cutting.	31
Figure 7. low speed wind tunnel.	31
Figure 8. Arduino uno board and setup that was used for the experiment.	33
Figure 9. Arduino setup with wing mounted in a wind tunnel.	33
Figure 10. Cl versus alpha graph demonstrating the pitching motion of the 21012 airfoil.	35
Figure 11. Cl versus alpha graph demonstrating the heave motion of the 21012 airfoil.	36
Figure 12. Cl versus alpha graph demonstrating the pitching motion of the 22012 airfoil.	37
Figure 13. Cl versus alpha graph demonstrating the heave motion of the 22012 airfoil.	38
Figure 14. Cl versus alpha graph demonstrating the pitching motion of the 23012 airfoil.	39
Figure 15. Cl versus alpha graph demonstrating the heave motion of the 23012 airfoil.	40
Figure 16. Cl versus alpha graph demonstrating the pitching motion of the 24012 airfoil.	41
Figure 17. Cl versus alpha graph demonstrating the heave motion of the 24012 airfoil.	42
Figure 18. 21012 wing at AOA= 0° & inlet velocity = 10 m/s	44
Figure 19. 21012 wing at AOA= 0° & inlet velocity = 17.5 m/s	44
Figure 20. 21012 wing at AOA= 0° & inlet velocity = 25 m/s	44
Figure 21. 21012 wing at AOA= 0° & inlet velocity = 40 m/s	45
Figure 22. 21012 wing at AOA= 5° & inlet velocity = 32.5 m/s	45
Figure 23. 21012 wing at AOA= 5° & inlet velocity = 40 m/s	45
Figure 24. 21012 wing at AOA= 10° & inlet velocity = 40 m/s	46
Figure 25. 21012 wing at AOA= 15° & inlet velocity = 10 m/s	46
Figure 26. 21012 wing at AOA= 15° & inlet velocity = 17.5 m/s	46
Figure 27. 21012 wing at AOA= 15° & inlet velocity = 25 m/s	47
Figure 28. 21012 wing at AOA= 15° & inlet velocity = 32.5 m/s	47
Figure 29. 21012 wing at AOA= 15° & inlet velocity = 40 m/s	47
Figure 30. 22012 wing at AOA= 0° & inlet velocity = 10 m/s	48
Figure 31. 22012 wing at AOA= 0° & inlet velocity = 17.5 m/s	48
Figure 32. 22012 wing at AOA= 0° & inlet velocity = 25 m/s	48
Figure 33. 22012 wing at AOA= 0° & inlet velocity = 40 m/s	49
Figure 34. 22012 wing at AOA= 5° & inlet velocity = 32.5 m/s	49
Figure 35. 22012 wing at AOA= 5° & inlet velocity = 40 m/s	49
Figure 36. 22012 wing at AOA= 10° & inlet velocity = 32.5 m/s	50
Figure 37. 22012 wing at AOA= 15° & inlet velocity = 40 m/s	50
Figure 38. 22012 wing at AOA= 15° & inlet velocity = 17.5 m/s	50
Figure 39. 22012 wing at AOA= 15° & inlet velocity = 25 m/s	51
Figure 40. 22012 wing at AOA= 15° & inlet velocity = 32.5 m/s	51
Figure 41. 22012 wing at AOA= 15° & inlet velocity = 40 m/s	51
Figure 42. 23012 wing at AOA= 0° & inlet velocity= 10 m/s	52
Figure 43. 23012 wing at AOA= 0° & inlet velocity = 17.5 m/s	52
Figure 44. 23012 wing at AOA= 0° & inlet velocity = 25 m/s	52
Figure 45. 23012 wing at AOA= 0° & inlet velocity = 40 m/s	53
Figure 46. 23012 wing at AOA= 5° & inlet velocity = 32.5 m/s	53
Figure 47. 23012 wing at AOA= 5° & inlet velocity = 40 m/s	53
Figure 48. 23012 wing at AOA= 10° & inlet velocity = 32.5 m/s	54

Figure 49. 23012 wing at AOA= 10° & inlet velocity = 40 m/s	54
Figure 50. 23012 wing at AOA= 15° & inlet velocity = 17.5 m/s	54
Figure 51. 23012 wing at AOA= 15° & inlet velocity = 25 m/s	55
Figure 52. 23012 wing at AOA= 15° & inlet velocity = 25 m/s	55
Figure 53. 23012 wing at AOA= 15° & inlet velocity = 40 m/s	55
Figure 54. 24012 wing at AOA= 0° & inlet velocity = 10 m/s	56
Figure 55. 24012 wing at AOA= 0° & inlet velocity = 17.5 m/s	56
Figure 56. 24012 wing at AOA= 0° & inlet velocity = 25 m/s	56
Figure 57. 24012 wing at AOA= 0° & inlet velocity = 40 m/s	57
Figure 58. 24012 wing at AOA= 5° & inlet velocity = 32.5 m/s	57
Figure 59. 24012 wing at AOA= 5° & inlet velocity = 40 m/s	57
Figure 60. 24012 wing at AOA= 10° & inlet velocity = 32.5 m/s	58
Figure 61. 24012 wing at AOA= 10° & inlet velocity = 40 m/s	58
Figure 62. 24012 wing at AOA= 15° & inlet velocity = 17.5 m/s	58
Figure 63. 24012 wing at AOA= 15° & inlet velocity = 25 m/s	59
Figure 64. 24012 wing at AOA= 15° & inlet velocity = 32.5 m/s	59
Figure 65. 24012 wing at AOA= 15° & inlet velocity = 40 m/s	59
Figure 66. Comparison between v-f behavior of 31015 and 34015 airfoils at 0° angle of attack	60
Figure 67. Comparison between v-f behavior of 31015 and 34015 airfoils at 5° angle of attack	61
Figure 68. Comparison between v-f behavior of 31015 and 34015 airfoils at 10° angle of attack	61
Figure 69. Comparison between v-f behavior of 31015 and 34015 airfoils at 15° angle of attack	61

Table of Contents

1) INTRODUCTION	1
2) LITERATURE REVIEW	14
3) METHODOLOGY	27
4) RESULTS & DISCUSSION	34
5) CONCLUSIONS	62
6) REFERENCES	64
7) APPENDIX	67
8) LIST OF PUBLICATIONS	71

CHAPTER - I

INTRODUCTION

What is wing flutter? Why does it occur? What is the necessity of avoiding wing flutter? To find the answers for these questions, one should know about aero elasticity. Aero elasticity is the science of understanding how a body behaves when aerodynamic loads show their impact on it.

Whenever a solid body is under a fluid flow there are three forces in the system; aerodynamic, elastic and inertial forces. When the study is concentrated on the impact of aerodynamic and inertial forces, it is called 'flight mechanics'. In the same way if the area of concentration is on the influence of aerodynamic and elastic forces, the study is called as 'aerospace structures' and when the area of interest is on the inertial and elastic forces, the science is 'Elasticity'. With all of that being said, the impact of all the three forces is what is called as aero elasticity. Aero elasticity can be classified again as 'dynamic aero elasticity' and 'Static aero elasticity'. There are several problems that were identified, when it comes to static aero elasticity as well as dynamic aero elasticity like Divergence, aileron reversal and LCO. Our problem of interest which is flutter is a kind of dynamic aero elasticity and body freedom flutter which is only dependent on the inertial as well as forming properties of the wing. This classification of aero elasticity can be clearly explained with the help of collars triangle (Figure 1).

Flutter is a self-excited vibration and this problem is faced by lifting surfaces in particular; this means that whenever a body starts producing lift, there is every possibility of the body to flutter. Not just in lifting bodies but whenever flow passes over a structure there is a possibility of flutter showing up and that is the reason why flutter has its own importance the field of turbines, where the turbine blades will flutter and flutter also takes place in civil construction, and there are historical evidences where the civil constructions start to flutter and got destroyed. When it comes to wing flutter it has gained its importance as the aircrafts the manufacturers started giving priority for lighter weighing materials. As the material is lighter there is a very good chance of the wing to flutter at lesser speeds, and this has turned the attention of the designers to concentrate on the field of aero elasticity and on the other hand if the

material is hard and stiff, it causes a serious discomfort for the persons travelling in the aircraft as the vibrations will start to reach the interiors of the aircraft.

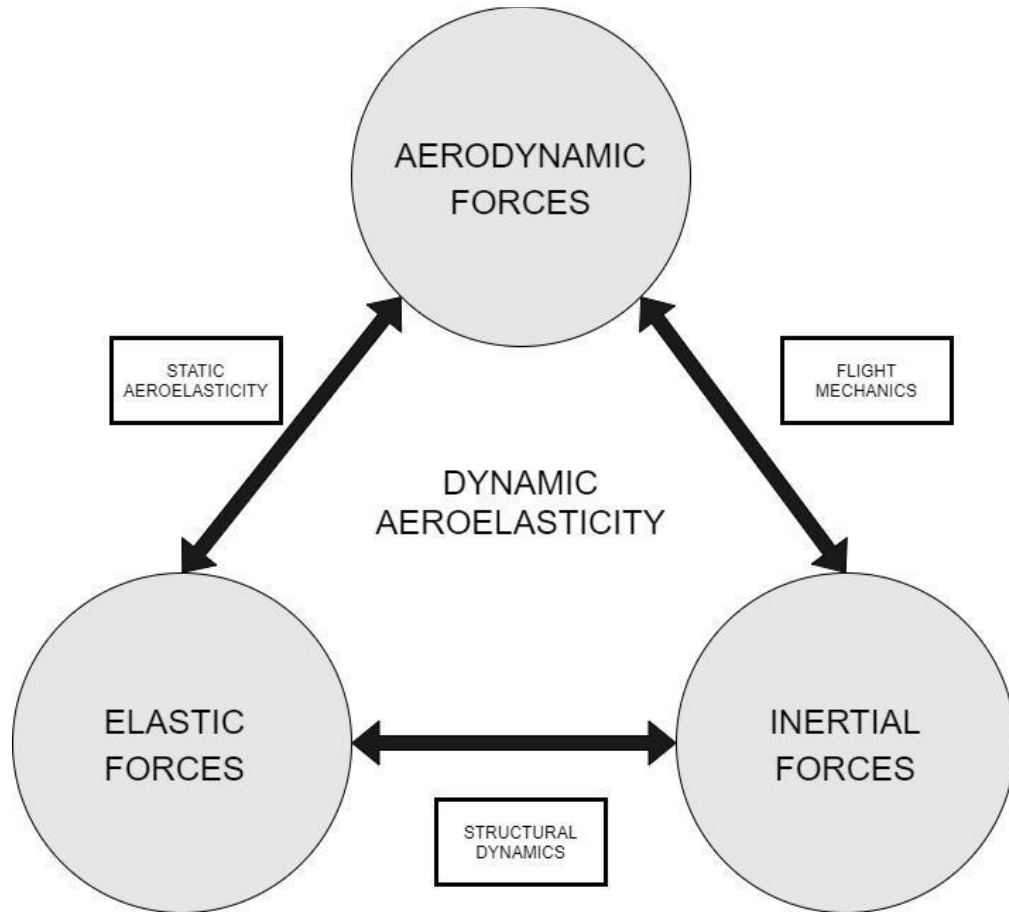


Figure 1 Collars triangle

Anybody under the influence of aerodynamic forces will start to vibrate at certain frequency and as the body keeps to move under the same forces, the vibrations will start to increase and will reach to a certain frequency where the vibrations will be uncontrollable and lead to rigorous vibration of the body and at a point the body will be shattered into pieces, and this phenomenon of the body vibrating at smaller frequencies, catching up to a rigorous and different frequencies which finally blows up the wing is what none can expect and happens in no time which is why flutter is called a catastrophic phenomenon.

In the wing flutter the body will start to have bending as well as torsion wise deformations happening at the same time and this kind of behavior is what is called as

‘classical flutter’ on the other hand, the wing will have only one degree of deformation which is torsion and this kind of flutter is what is called as ‘torsional flutter’. These are the two basic flutter types that were studied.

The wing will start to flutter after the aircraft reaches a certain speed and the speed at which the body starts to flutter is called flutter speed; the higher the flutter speed of the body is, the later the body will start to flutter. When this is achieved, it could be a success as in this case the flutter was delayed. It is very important to study the mode shapes of the structure in order to understand the flutter of the wing as the combination of two or more mode shapes will cause the wing to flutter, and flutter modes can be identified if a couple of often more mode shapes are seen to combine or seem almost to combine.

Airfoil Nomenclature:

Location of maximum camber is taken as the parameter

What influences wing flutter?

Many researches were done to understand the effect of various parameters that include aerodynamic parameters, topological parameters, loading conditions, various design parameters and various other issues and values of the aircraft and their influence on the flutter behavior of the aircraft was studied and identified.

In this part of the chapter we will discuss the effect of selected parameter or value on the flutter of a wing. It should also be understood that it is hard to cover all the parameters that the researchers have covered hence only a certain selected parameter will be highlighted in the following content.

Aerodynamics: When it comes to the aerodynamic values that influence flutter, the drag which is an unavoidable force for body under a flow, drag can significantly reduce the critical speed for wings with a very high aspect ratio, while improving the critical speed for wings with average or regular aspect ratios, will improve the critical speed for wing with average or regular aspect ratios (1). When it comes to the aeroelastic behavior in the transonic regime, it is much more complicated and difficult to analyze due to the dynamics of shock waves and the separation of the boundary layer,

which are key parameters (3). Whenever an additional weight adds on to the structure, its inertia will definitely be affected because of the added weight. So studying the flutter characteristics of a general wing without any added weight like that of a real model might not give results that can guide for designing a practical wing. This as an idea of study, analysis was performed for flutter on a wing while adding forces due to thrust, store mass and the interfering of these forces with the aerodynamic loads. Hamilton's principle of variation was used to derive the equations of motion as well as boundary conditions. A twin jet wing where the engine close to root being called as first engine and the engine far from root as the second one was considered and for different permutations of position of engine over the wing was considered both for chordwise as well as the distance from the root of the wing along with different values of thrust from each of these engines or from both of these engines was taken into account. The second engine was considered at a distance of 70% from the root and chord wise position to be at 25% aft the leading edge, based on the thrust values of second engine and selected values of trust from first engine the flutter boundary was calculated and it was observed that there was a decrement in the flutter speed continuously along with the increase in follower force. Total of four cases were analysed, the first being both engines are turned off, the second case and the third case when only either of the two engines are working and in the same way the fourth case is when the engines are considered to be turned off, there will be no follower forces instead engines can be considered as two weights. After performing the analysis, it was noted that the flutter frequency was lesser for any considered value of thrust, as the engine mass increased [5].

Coming to the influence of changing the engine positions over span of the wing, when the first engine is placed at 30% from the root and when the position of the second engine was changed from about 50% of the span the wing to almost closer to the wing tip, it was that when the first engine is placed at 30% from the root the optimum position of the second engine is at 70%. In the same way it was also observed that for a twin engine wing was better in terms of stability compared to a single engine wing. [5].

Shape: As the aerodynamic performance of the wing is influenced by the shape of the aerofoil and as the aerodynamic properties of a wing will definitely impact the

aero-elastic characteristics of the wing, the flutter characteristics of the supercritical aerofoil needs to be understood. When compared to the conventional aerofoils, the supercritical aerofoils will have greater coefficient of lift and also as the sonic speed is obtained, for a supercritical aerofoil we can observe that the rise in drag will be hampered. By studying the dynamic pressure that was calculated at the flutter frequencies, it was evident that the wing with conventional aerofoil have lower dynamic pressures in subsonic regimes as compared to the wings with supercritical aerofoils. After comparing the analytical and experimental results, it was concluded that the natural vibration modes that will combine to cause flutter were similar for both types of wings. These results were concluded based on the wind tunnel experiments on the wing models that were constructed in such a way that both the wings will deform at a particular value of dynamic pressure as well as mach number (2). When an analysis is performed for the influence of inertial and forming properties on the body freedom flutter of a wing is performed, a beam model was considered as it is easy to model and analyze compared to the finite element analysis models. NACA 0012 aerofoil was as wing profile and simple I beam with skin was use as model and is analysed in Natasha application. To calculate the effect of engine and fuselage, the mass and inertia of the fuselage was added on nodes at reference points and engine was also added at reference points at equal distance from both sides of the wing. The strip theory of aerodynamics is used by NATASHA. The results proved that the total mass, inertia of the fuselage and location of centre of gravity of the fuselage seem to influence the body freedom flutter of the wing. Out of the listed parameters, it is clear that inertia of fuselage increases with increase in mass of fuselage. To understand the impact of both inertia and mass of fuselage separately, the inertia was kept constant while varying the fuselage mass. From the results it was concluded that when inertia of the fuselage was the only incremented parameter, a increase flutter speed was observed but when mass was increased, a decrease in flutter speed was seen. it can also observed that location of centre of gravity has influenced flutter highly this was concluded when the location of centre of gravity was varied longitudinally to aft of the wing, it was clear that for moderate change, the flutter speed was lowest (3). Incorporation of winglets and changing shape of wing will help in improving Aerodynamic properties

of the wing. but that will definitely show some impact on the aero elastic behavior of the object. C-type winglets and its effect on the flutter behavior was studied which can guide in understanding the impact of winglets on aero elastic behavior of the wing. according to previous research, addition of winglet reduced flutter speed which could be due to additional weight on the wing. computational fluid dynamic analysis and general finite element method program was used and both of them were coupled which is called fluid structure interaction analysis to get required results. 'models for aero elastic validation research involving computation' in short 'mavrik' ring model was tested in transonic tunnel on a typical business jet configuration. Based on analysis and validations it was found that the stiffness of winglet was having a minimal impact on the wings flutter whereas the mass and aerodynamics of the winglet played their roll on the flutter characteristics. Especially the winglet aerodynamics especially has high influence in reducing speed and incrementing the flutter frequency (7).

Structure: Another study was performed for understanding the effect of connections that are used to attach the engine the wing, and the engine was assumed as unbalanced weight. The wing model was considered to be having degrees of freedom in 5 directions. The wind model was along with flap and balanced weights which resembles that engine in real model and this model was tested in wind tunnel such that the angle of attack can be changed so can the dead weights. The wing was modeled with ribs to resemble the real time being and an engine with propellers that have an unbalanced mass was mounted on to it. Care was taken such that the wing could move in plunge and vertical directions also, springs and dampers were used for this sake. Initially experimental analysis was performed and some of those values were used for numerical analyses. From the results it was concluded whenever the engine mass was increased introduction in the flutter speed was observed in the system irrespective of the thrust values. If the thrust values were considered, it was seen that as the thrust was increased a decrement in the flutter speed took place, this happens because whenever thrust is increased, it will destabilize the wing and will force flutter to occur at lower speeds itself (4).

Material: If the ratio of torsional rigidity to the bending rigidity is considered to be '1', if the value of 1 is 0.02 and 1, the growth in the value of drag has shown to improve the flutter behavior of the wing and if the value of '1' is considered less than 0.02, the flutter stability was observed to be lowering and if the ratio of torsional rigidity to the bending rigidity '1' is seen as 1, it was observed that the bending frequencies and torsional frequencies seem to cross over each other without being coupled to each other (1). When the wing is manufactured with flexible material, torsion and bending torsions will get coupled and will direct to an effect known as wash out where angle of attack will become reduced as the wing gets twisted. On the other hand, when a rigid wing is compared with a flexible wing taking the mach to be transonic, it was observed that a single shock has formed on the rigid wing and when it comes to a flexible wing, two shocks were formed. As a result of the formation of two shocks on the wing even if the angle of attack or mach number were incremented to a very minimal value, both shocks seem to travel against each other and were observed to be merging at higher mach values. For selected values of force amplitude of an unbalanced mass mounted engine were studied for the effect of the mass of the engine on flutter speed and flutter frequency of the system. When an engine with unbalanced mass was used, a reduction in flutter frequency and speed was observed when engine mass and force amplitude of unbalanced engine was increased. Here the unbalanced force acts as a source of instability over a period of time. In the same case of unbalanced force, perpendicular distance between the wing and engine was increased, reduction in flutter speed happened (3). With the aim of achieving higher endurance and improving the flight envelope, lighter and Slender wings that are manufactured with advanced composite materials are desired so that a reduction in structural weight as well as enhanced aerodynamic performance can be obtained. A chord wise flexible NACA 0024 airfoil that is manufactured with composites was studied to understand the influence of stiffness and density of composite plates on flutter behavior and also for the possibility to improve flutter boundary depending on the aero elastic configuration of the system. The density was calculated by measuring mass at known surface area and stiffness was measured depending on the response to disturbances. To perform a wind tunnel experiment, a hello speed wind tunnel with an open circuit with maximum velocity of

28 meters per second was used. Critical flutter speed had a noticeable improvement in bimodal behavior of the aero elastic system at greater pitch versus plunge frequency ratios (6).

Efforts to Suppress or Delay flutter:

Many researches were conducted to discover different methods to either suppress the flutter or to find a way to delay its occurrence. In this part we shall try to get a glance of different methods that were explored and tested to get the desired output. The parameters that were found to have impact on the flutter were tried to either control or reduce the effectiveness of the influencing parameters.

Flutter can sometimes be controlled with the help of control surfaces that are incorporated in any traditional aircrafts by altering the aerodynamics. One of the feasible ideas was to incorporate a dynamic vibration absorber that can control vibrations in the wing when a particular frequency was reached and this method seem to improve the flutter speed by almost quarter times and in the same way when a closed loop active DVA was implemented, it showed a better results that was almost half times effective than a regular dynamic vibration absorber in improving the flutter speed (8).

Morphing wings, which is the current trend in the field of materials, were also tested for their effectiveness in controlling the flutter of a wing and was showing better results. A span-wise morphing wing was tested for its impact on the flutter of the wing with morphing rate and span length as key parameters of interest. These parameters were proved to play their role in the flutter behavior of the wing as the critical flutter speed seems to be getting lower as the span was expanded and seems to grow as the rate of morphing was increased (9). Another experiment of this kind was about using shape memory alloys (SMA) as an integral part of the wing to control the wing flutter. The shape memory alloy was used to stiffen the wing as there was increase in vibration. As the vibration increases, there will be a vibrometer that will measure the vibrations and will signal the material to change its shape and make the wing stiff. Even this method has proved to be effective in controlling the wing from fluttering (10).

So in this chapter a brief of wing flutter was discussed along with the reasons and controlling methods that seem to be effective in controlling flutter. This chapter

will help in understanding how flutter will confine the designers in many aspects and also about how these were tried to control.

Static Problems

The steady-state aerodynamics of elastic bodies are taken into account. The transfer between aerodynamic and elastic forces can show a tendency to diverge in highly flexible structures, ultimately leading to failure. On the other hand, if it is stiff enough, a stable equilibrium will be established. Overall, these issues can be categorized as follows: Divergence, aileron effectiveness, lift distribution, and static flight stability.

Divergence occurs when the lifting system suddenly deforms to the point of failure after reaching critical speeds. As the speed increases, the torsional centre lift and torsional moment also increase. This increases the local angle of attack, which also increases lift. Above a certain speed limit, divergence speed, and torsional stiffness of the structure, the aerodynamic moments become unbalanced and unstable. This problem is called torsional divergence. Other deviations are possible in theory, but historically this is the significant deviation. Another case occurs in the presence of roll motion control, ailerons, which provide additional lift to the wingtips near the trailing edge. Deflection of the ailerons so that the additional lift is directed upward creates an additional moment that twists the nose downward and reduces the local angle. This reduces the effectiveness of the control surface. Again, the aileron deflection does not generate any roll moment from a given speed, the aileron reversal speed. Finally, lift distribution is the effect of elastic deformation on aerodynamic pressure distribution, which of course is included in the divergence problem. Static flight stability is the effect of elastic deformation on aircraft controllability, static margin or control behaviour.

Dynamic Problems

When the situation becomes time dependent, we enter the realm of dynamic aeroelasticity. This is related to unstable structural vibrations. Flutter probably affects high-speed aircraft most extensively. The classic type of flutter is associated with latent flow, usually he involves coupling two or more degrees of freedom (DOF). Non-

classical properties of flutter may include discrete flow, turbulence, and stall conditions. Below is a brief description of each issue.

a) Bending and torsional connections:

This is a classic two-degree-of-freedom flutter where bending and torsional modes coalesce. Pure bending or pure torsional vibrations dampen quickly, but when combined and phase-shifted by 90° , abrupt self-excited flutter occurs.

b) Dynamic Flight Stability:

This section only refers to the effect of elastic deformation of the structure on the dynamic stability of the aircraft.

c) Buffets:

This is most caused on horizontal stabilizers by vortices created by poor airflow in the wing trail. If their frequency is equal to the natural frequency of the tail, resonant vibrations can occur.

d) vibration shock:

Nonlinear effects of compressible flow in the presence of unstable shock waves.

e) User interface humming:

This phenomenon is also a shock wave near the hinge in front of the control surface (but here in the transonic regime). Surface deflection changes the strength of the impact, which in turn changes the boundary layer pressure behind the impact. The result is a sucking/pushing effect on the controls and possibly an undamped swing.

f) Supersonic disk flutter:

Panel flutter is the self-excited vibration of the skin of an aircraft as air flows along the surface of the aircraft. At supersonic speeds, skin plate temperatures can reach hundreds of degrees, resulting in large heat excursions.

g) Vortex shedding:

A phenomenon commonly known in flows around a cylinder, where the wake becomes unstable with increasing velocity and fluctuations in eddy strength give rise to von Karman vortex streets. Forces and moments on the object fluctuate along the flow and vibrations are induced in the object. This is important, as it can also occur, for example, in turbine blades with a high angle of attack.

h) Stall flutter:

This is more likely when the blade or airfoil is heavily loaded (near stall condition) and off-design conditions occur that can cause self-induced divergent vibrations.

i) Memory flutter:

If large external objects such as engine nacelles, fuel tanks, guns, etc. are attached to the wings of an aircraft, the dynamic characteristics, especially the flutter speed, can be adversely affected.

j) Eddy flutter:

This problem typically occurs on tiltrotor aircraft. In high-speed on-axis flight, the large influx through the rotors creates significant forces on the plane. These forces interact with pylon/wing motion and can destabilize the system.

k) Body Freedom Flutter:

Body Freedom Flutter (BFF) occurs primarily on the lift surface and results from the coupling of rigid-body longitudinal dynamic modes, called short-term modes, with wing bending.

Fluid-Structure Coupling

In the previous chapter, we briefly described the governing equations of both domains involved in all aeroelastic phenomena in liquids and solids. Especially in the fluid mechanics section, some approximations were given and the results discussed. This chapter covers two parts, the so-called fluid links and influences.

Structural interaction (FSI). The FSI problem has his three main challenges:

Problem formulation, numerical discretization, fluid-structure interaction. The first two is about domain conditioning and approximation. Here we discuss the remaining issues arising from two different subsystems. He can divide the problems of fluid-structure interaction into two classes: Monolithic and Staggered.

Monolithic Approach

The model simultaneously solves fluid, structural, and mesh motion equations. A fully integrated FSI solver is described here with improved robustness. However, such an approach can be very difficult to implement for large-scale problems. The three categories of strong coupling techniques are:

- Block Iteration Coupling – Fluid, structure and mesh systems are treated as separate blocks and non-linear iterations are performed block by block.
- Quasi-direct coupling – Same idea as block iteration, but the fluid and structural equations are connected within the same block.
- Direct Connection - Since there is only one block, all variables are connected by a set of equations.

Frame of Reference

The first question comes from the frame of reference, in order to be able to solve all areas simultaneously. The Eulerian (or space-fixed) coordinate system is typically used to solve fluid flow, while the Lagrangian (or material-fixed) coordinate system is used for structural problems. For both liquid and solid aeroelastic problems, neither formulation is optimal for the whole spectrum. Also, the combined algorithm becomes very complex when it has to deal with Lagrangian networks that overlap Euler networks.

The most used solution is the arbitrary Lagrangian-Euler (ALE) method. This allows the mesh to be moved in arbitrary ways and reduces the two limiting cases to Lagrangian and Euler formulations.

Added-Mass Effect

In fluid mechanics, a body and a fluid cannot occupy the same physical space at the same time, so the body that is accelerating or decelerating has to move some of the fluid around it, so the extra mass is added to the system.

This problem occurs in the iterative process of monolithic schemes. In applications such as blood flow, fly worms, or parachutes, where the fluid density and structure are comparable, the effect of added mass can destabilize the scheme. It does not affect aircraft wings.

Staggered Approach

Nonlinearity of the fluid equation (for Navier-Stokes or Euler equations). Structural equations, on the other hand, can be linear or nonlinear. Such situations can result in matrices with varying properties, making the solution process difficult. Hence the monolithic Schemas are generally computationally intensive, mathematically and economically suboptimal, and cannot be managed by software. Alternatively, fluid and structural mechanics equations can be solved by a step-by-step procedure. Such algorithms typically solve the fluid dynamics using the velocity boundary conditions from the previous step, then solve the structural equations using the updated fluid interface loads, and then, for a given time step, We need to solve the mesh motion using the new structural displacement. When structural or extra mass effects are applied.

Having defined both a structure solver and a flow solver that are completely independent of each other, it is clear that the hierarchical approach is the only option. Some common schemes for transferring results between subsystems, including using parallel computing capacity. For this work, we will stick to the simpler and more general serial method.

CHAPTER – II

LITERATURE REVIEW

Incompressible, viscous stream over a reformed 0015 airfoil of NACA four-digit series is united with a two level model of a adaptably upheld airfoil. Projected the notion of energy separating method which practices the plunged limit approach program ViCar3D shaped. Three key limitations are examined: the reduced speed, the equilibrium method, and the area of the hinge point. Mathematical examination is achieved using the energy separating plan. The effects integrate computational models of stream motivated diving gestures of 0015 airfoil of NACA four-digit series have been finished at $Re=1000$. A parametric exploration of pitching response volume of agreement point-of-attack, reduced speediness, and area of elastic hinge is accounted for. It is seen that increasing the agreement tactic reduces the basic & amp; at which the background gets unpredictable to accurate irritations. Additionally, the outline loses recollection of the equilibrium approach for huge abundance signals. An study of the outline's affectability to the part of the elastic pivot presented outcomes that were to a boundless level in harmony with the inert airfoil balance estimates, a authority allocating scheme was useful to an instance of a diving airfoil and it reveals the size to take separately the obligation of unlike twisters to the efficient rules on the airfoil [11]. The study was unequivocally initiated on the checkup of consequences amid computational examination complete using ANSYS CFX and investigative practice. The Aero elastic Prediction Workshop (AePW) stretches a convenience to estimate complex computational plans and devices for forestalling aero elastic aces. Two circumstances were focused to legitimize the products. The main case joins reliable and forced convincing tried in the NASA Langley Transonic Dynamic Tunnel using the Oscillation Turntable (OTT) workplace, and second state where wing trembling irritated in the TDT on an flexible base pitch and plunge powered assembly which provides two level of-opportunity lively measure. A sure explanation is given in respect to the sample method to the wing shudder examination. A listed representation in regards to the lattices used for CFD designs is provided. An enormous opinion by opinion association among the assessment outcome and controls are explained by applying graphical plans which use numerous simulations like SST, SST k-w, SA, and

so forth these simulations similarly vary about the time-steps per period is disturbed. RANS and URANS power coefficient prediction plans are used in the Ansys calculation for creating the specific persistent influence figures for association with the trial ones. Spatial grouping with static improved time-step-size of $128\Delta t$ and instable outline scope display affectability to force coefficients. Lift coefficient types regardless of the reality that highly little are visible regarding matrix refinement. Drag and 2nd coefficient suggests extra distinguished affectability with matrix refinement, and the types are monotonic. The exploratory FRFs of urgent thing greatness and level are contrasted and the computationally were given FRFs at 60% wing-duration place. The length FRFs show affectability to lattice refinement on the fundamental sights pinnacle district, with medium and great matrices foreseeing closer consequences. Lower floor urgent thing volume FRF at 60% wingspan suggests first rate healthy with tests, and not using a lattice affectability [12]. The number one factor of the paper is to research the concept of the aircraft for the duration of the vacillate of subsonic traveller aircraft at its journey pace utilising development gadgets like CFD and FEA tools. A new exam known as Fluid layout cooperation known as FSI. The research is carried out of how the aircraft wing shape will disfigure in regard to circumstance. The wing is deliberately utilising programming and broke down utilising Ansys workbench. The consequences are checked out among singular research and consolidated FSI analysis. The paper suggests methodologies for direct underlying methods wherein the elevated strength performs at the point of interest of urgent things and the exam is completed. The method proposed i.e FSI demonstrates to expose greater unique effects than singular exam. Likewise, from the effects we will realize the numerous mis happening for unique mode shapes. It is completed by pronouncing that the FSI is an excessive degree method for dissecting the wing [13]. The number one concept of this paper is to examine the frequencies, coefficients of urgent thing and pace of liquid/air received each tentatively and computationally. By utilising the concept of take a look out and plunge there via means of differing the pitch and top of the version stored with inside the air circulate there via means of converting the velocity of air to make the vacillate surprise for acquiring exploratory effects. Utilization of ANSYS multiphysics (MFX). This module changed into basically produced for liquid creation affiliation contemplates. On one

side, the number one element is addressed utilising ANSYS Multiphysics and at the contrary side, the liquid element is tackled utilising ANSYS CFX. A nitty gritty explanation is given regarding the extrude of move sections among the underlying and liquid lattices. The ANSYS code is going approximately because the professional code and peruses all of the multi-place orders. It recovers the interface lattices of the CFX code, makes the making plans and conveys the limits that manage the timescale and coupling circles to the CFX code. A NACA 0012 airfoil changed into applied and the development changed into simply approved a solitary DoF, i.e., in twist. A concord duration of eight inches and a pointy aspect duration of 21 inches had been applied. The wing changed into produced from an aluminum shell of 1/32 crawls in thickness. A spring consistent of 5.826 Nm/rad changed into applied. The recurrence present other than the whole lot else in a specific pace variety is talked approximately as extra increment in that attain introduced approximately mathematical calculation constraints. For this situation, it is going to be greater difficult to determine the vacillate pace because the airfoil accomplishes concord with inside the gradual down quarter with the circulate pace genuinely expanding. This article pondered at the dissimilarity and 0-recurrence ripple marvels. The ANSYS-CFX coupling to illustrate liquid layout conversation has been extraordinarily beneficial and we've got had the choice to agreeably show those wonders interior limits constrained via way of means of computational restriction. It seems to be that the restriction amongst disparity and ripple is extraordinarily restricted. The demonstrating of such marvels is extraordinarily thoughts boggling and we see that it is, still, difficult to supply closely reproducible effects. The trouble lies in computational limits and, additionally, some refinements to be introduced into clinical showing [14]. A NACA 64A006 ordinary and a MBB A-three supercritical airfoil had been studied. Both the steady and insecure streamlined coefficients had been processed via way of means of utilising LTRAN2-NLR code. Flutter and time-response investigations are done for a NACA 64A006 normal and a MBB A-three supercritical airfoil, each wavering with plunge, pitch, and aileron pitch ranges of-opportunity (DOF's) in little aggravation transonic circulate. The streamlined coefficients are decided utilising the transonic code LTRAN2-NLR. The influences of various varieties of aero elastic barriers on vacillate speeds for the bowing twist, bowing

aileron, and twist aileron branches are examined. The ripple speeds associated with the twisting twist branch are plotted in opposition to Mach numbers for diverse boundary esteems and the transonic plunge surprise is illustrated. To remember the shudder modes, the ripple pace, sufficiency percentage, and level difference at diverse mach numbers are plotted in opposition to the mass percentage for each a 2DOF and a 3DOF case. Time-response consequences are received for the NACA 64A006 and the MBB A-three airfoils at $M=Q$. eighty-five and 0.765, individually. For the NACA 64A006 airfoil at $Af=0.7$, impartially solid reactions had been received depending on a gaggle of boundary esteems evaluating to a shudder circumstance in a unique vacillate analysis. The wonderful headway of the aileron mass attention can't simply dispense with the ripple limits of aileron associated branches but similarly accelerate the twisting twist branch. The impartially solid reactions had been gotten whilst the flight pace changed into reduced via way of means of three.5% [15]. The airfoil houses become aware of with in step with unit duration which essentially remains something very comparable at any optional area of the element alongside the attain. Here c is the congruity duration of the airfoil, h and α suggest the heave (wonderful vertical) and pitch (wonderful nose up) moves one after the other of factor O . X_{cp} , X_{cm} and X_o are the spots of focal factor of compacting thing, factor of convergence of mass and focal factor of flexural rotate independently. The move phase close to the restrict of airfoil is stored higher due to the presence of better incline of circulate houses (p , ρ , T , V) and roughness influences close to the airfoil floor whilst stood out from the out of doors furthest reaches of circulate domain. The loose circulate restriction situations implemented on the upstream of the distance are u_∞ v_∞ ρ_∞ and p_∞ but 0 squeezing thing restriction circumstance is implemented on the downstream of the distance. Different limits portrayed in FLOTRAN CFD solver for tending to circulate over an airfoil like fluid houses. At that factor, the additives of NACA 0012 airfoil, with without a doubt crucial damping, are focused below unique breeze circulate situations. The consequences are received via way of means of coupling ANSYS FLOTRAN with the in-residence crucial code in time area the use of the Newmark's computation. For a given methodology, FLOTRAN re-enacts the squeezing thing scattering over the airfoil that's accordingly used to sign up the smoothed out elevate and moment. These elevate

and 2nd is then handed to the crucial code to evaluate the reaction of the airfoil. Here, the cost of crucial damping extents $V_h = 0.01$ and $V_a = 0.01$ are notion of. The time records of the tremendous reaction (fling and pitch) of the airfoil on the signal of assist and the pertaining to smoothed out elevate coefficients for diverse loose circulate wind modern paces had been inspected it is visible that the throw additionally, pitch traits and the pertaining to smoothed out elevate coefficient have an impact on and be part of to 0 suggest situation of the airfoil with time at circulate pace of one hundred ninety m/s. Obviously on the circulate pace of 192.forty five m/s, each the heave and pitch traits of the airfoil are essential consonants in nature and their amplitudes live steady with time. This pace is the waver pace of the airfoil system. It has a tendency to be visible that at a circulate pace of 193 m/s, the airfoil falters unboundedly whose amplitudes boom extensively with time. The consequences on this way show that the moves of the airfoil at below-modern velocities lower than 192.45 m/s is steady, and people preceding this essential pace are unpredictable [16].

In the examination with the aid of using Razak, Norizham and Andrienne, the aero elastic reaction is determined on the NACA 0018 wing. The foremost reason for this studies is to examine the wing present process stall flutter in the pitch diploma of freedom. Stall flutter is essentially the restrict cycle oscillation due to the periodic waft separation of the wing withinside the uniform waft. The wing is analyzed for one of a kind velocities and one of a kind angles of assault. The waft of the wing is determined with the assist of particle photo velocimetry. The wing is constant horizontally in a wind tunnel to a beam related to springs. The wing is analysed for one of a kind velocities and one of a kind angles of assault. The selected angles at which the airfoil was tested are 110,120,130,140,160 stages and the selected velocities variety from 8m/s to 25m/s. The dimensions of the wind tunnel is 2m x 1.5m x 5m. The waft is visualized with the assist of particle photo velocimetry and the rate is calculated from the PIV software. The Images of the waft are taken from the CCD digital digicam. The acceleration and strain values are taken from the sensors. The strain distribution is drawn from the calculations of the strain faucet connections. The strain and accelerations are determined for one of a kind airspeeds and angles of assault. The take a look at setup includes a low-pace wind tunnel, beams and springs and laser supply

i.e., PIV equipment. The strain and acceleration sensors had been used for LCO plotting, CCD digital digicam became carried out for imaging the waft and the Pressure-faucet connections had been used to take a look at the strain distribution. The graphs had been plotted among the airspeed and the pitch amplitude; facts from the 12-diploma configuration display that the bifurcation to LCOs takes place at a decrease airspeed and the fold is determined at 13-diploma configuration. For the 14-diploma perspective of assault the important pace is 13.3 m/s.; amplitude vs time graph is drawn for each perspective of assault. The bifurcation conduct is studied for NACA 0018 wing for each perspective of assault. Lower static angles result in better onset LCO speeds inflicting LCO amplitudes developing exponentially. From the PIV it is determined that the waft separation takes place at the top wing only. The main area vortex is determined. At intermediate angles of assault, the fold bifurcation passed off, inflicting hysteric leap in LCO amplitude. As perspective of assault and pace increases, the bifurcation conduct additionally changes, the experimental model was created to test the flutter response and stall flutter properties of the wing in the wind tunnel at the University Of Liege, Belgium. Instead of rods, linear springs were used to describe the pitch and plunge stiffness of the wing in this experimental model. The tests were carried out on NACA 0018's wing's Pitch and plunge motion were measured using accelerometers. Oscillations in the high and low limit cycles were noticed and the real instantaneous velocity on a single plane parallel to the free stream velocity was visualized. Experiments revealed sharp-leading-edge stall flutter behavior caused by vortex shedding and the formation of a laminar separation bubble at the leading edge [17]. Another study carried out with the aid of Tang, Deman & Dowell on aero elastic instabilities and the reasons for structural failure of two diploma of freedom flutter is a aggregate of torsion and bending modes. To take a look at the flutter, a flutter mount device has been developed. The dimensions are decided from the finite detail and verified with the aid of using the aero elastic model. To decide the mode shapes ERA, an identity set of rules is used. Frequency reaction features are received and v-g-f graph is plotted. Natural frequency, pitch stiffness and plunge stiffness are decided with the aid of using the finite detail evaluation. The speed of the wind tunnel is saved various to take a look at the flutter reaction. Frequencies are decided with the aid of using the

ERA set of rules. The acceleration values are decided by the usage of the sensor on the center of the wing. The most speed of the wind tunnel is 50m/s. NACA 0012 2-d wing is constant on a mount device. The velocities and angles of assault are saved various to take a look at the flutter reaction. The Eigen device Realization Algorithm is used to decide the shapes of the first bending and 1st torsion. The Plunge vs time and the pitch vs time graphs are plotted to take a look at the dynamic instability of the aero elastic flutter. The Deflection vs time is the enter sign given throughout the identity procedure and the pitch and plunge vs time are the output plots. The Damping issue vs speed graph is illustrated to examine the traits of flutter. The Mount device is outfitted under the take a look at segment of the wind tunnel and the electrical motor is constant on the mount device to force the trailing area flap; it has an encoder used to degree the actual angular function of the flap. The ERA set of rules is used to decide the mode shapes. The Mode shapes are one of a kind for one of a kind velocities and the height of the mode shapes is converting as the rate is various. The pitch and plunge are getting coupled at 1.5Hz frequency. The values of damping issue for the pitch pace are slighter scattered in comparison to the plunge type. The dynamical capabilities of the elastic base association and the stiff wing had been showed with the aid of using an experimental Modal Study. The wind tunnel trials had been organized for validating the increase of the modes contributing to flutter with developing pace till the flutter attainment. The v-g-f graph suggests the evolution of the mode shapes of the flutter and frequencies, Chung presented an incremental technique for solving aero elastic issues with free play. Using the NASTRAN software and research has been done regarding data (mode shapes, natural frequencies, and damping) collected from ground vibration measurements, Pankaj developed a system for estimating the flutter characteristics of an aircraft construction. Hasheminejad used the Runge–Kutta technique to compute the open-loop supersonic aero elastic behaviour and flutter motion of a rectangular shaped and sandwich plate that has been elastically supported [18]. The flutter is a violent instability which could motive structural failure. If a plane is to perform then flutter clearance is a have to. In this examine the flutter in an aerodynamic surface (horizontal tail) is studied. If a plane is to perform then the flutter clearance is a have to. The layout is optimized computationally and evaluated experimentally. i.e., a hybrid technique is

observed to clear up the problem. The layout necessities given to the plane tail fashion dressmaker is to have the flutter pace better than 410 m/s. Later it became changed to 420 m/s however the computed flutter pace via whole finite detail evaluation is 378 m/s; finally, in order to suppress flutter, the flutter pace have to be 400m/s. the longitudinal and lateral region for saw-teeth designed tail is calculated. First, the layout is optimized computationally. Three saw-teeth designs are examined in a wind tunnel. Two units of gauges are established in torsional springs to calculate the flutter frequency. The facts is received from DAC i.e., facts acquisition card. The floor vibration takes a glance at is likewise done to decide the flutter frequency. Then the saw-enamel is eliminated and the process is repeated in low-velocity wind tunnel. The balanced mass of 4kg is used on this check. The device used on this test is the wind tunnel for checking out and the finite detail technique in computation for layout optimization. Data acquisition card is used to measure the flutter frequency. The floor vibration check device is used to measure the flutter frequency. Balanced loads are used to suppress flutter. Computational outcomes show that 10% growth in flutter velocity is viable. The flutter velocity is more desirable for saw-enamel layout and the development recorded was simplest 7% that is much less than the computational outcomes. One of the saw-enamel fashions gave higher outcomes however it shifts the enamel factor which places extra paintings on actuator. From this studies it's far concluded that increasing the damping frequency led to the flutter suppression. The Mass balancing and relocation have a tremendous effect on the flutter suppression. The Saw-enamel layout may be followed due to the fact it's far fee powerful however the lower in tail floor region shift the enamel factor so the actuator ought to get replaced which now no longer simplest provides extra fee however also is a? time-ingesting process [19]. In this paper the flutter evaluation of 2-D is defined. The flutter pace and flutter responses are recorded. The lengthy endurance UAV (NACA 2415) is constant withinside the wind tunnel check phase that is adaptably braced in pitch and plunge mode. Readings have been taken from the meter cabinet. The wing is primarily based totally at the 2-D mathematical version. The bending and torsional stiffness are calculated the use of ANSYS. Finally, the flutter pace is envisioned experimentally. The flutter reaction is evaluated the use of the spring and mass version and the plunge

stiffness is evaluated through the 2 linear springs constant to the cantilever beams through varying the operative span of the beam; the pitch stiffness is evaluated through the torsional springs. The situation for the flutter is checked and the end result deduces the use of the graphs for bending stiffness and torsional stiffness in ANSYS. The modal frequencies are calculated for the first 10 modes and the flutter is determined. Stiffness vital at better speediness of UAV a hundred and sixty knots is plunge: 521.90N/m, pitch: 1.983 Nm/radian, first bending frequency: 5.489Hz and primary torsion frequency: 26.940 Hz. The outcomes show that the flutter isn't found for the max wind tunnel velocity of 40m/s however at 240 knots. The ANSYS outcome shows that the flutter is found for frequencies in 1st bending and 1st torsion. The wing has an ok protection border to expose flutter past 240knots [20]. The aero elastic behaviour of the square wing in pitch and plunge mode is defined on this study. The square wing is subjected to exceptional airspeeds and angles of assault and the frequency reaction is found through the changes in strain, acceleration and particle photograph velocimetry dimensions. The restrict cycle oscillations are found for the leading and trailing area during the stall. The incidence of the trailing area separation is extra every day and had the tendency to stabilize the amplitudes of restrict cycle oscillations. The selected angles of assault for this test are 110, 120, 130, 140, a hundred and sixty and the air velocity ranges from 8 to 25.2 m/s. The accelerometer and strain sensors have been used to observe the frequency reaction. The rapid Fourier remodel is used to convert the time area into the frequency area. The go with the drift is visualized by the use of the PIV measurements. The wings taken into consideration are NACA 0012 and NACA 0018. The wing is fitted horizontally to the arm connected to springs. The laser supply is positioned beneath the version. The acceleration and strain values are drawn the use of sensors for exceptional air speeds and exceptional angles of assault. The time area is transformed to frequency area the use of FFT. The stall residences are found the use of the go with the drift visualization approach i.e., the PIV technique. The device used is the wind tunnel, linear springs, aid beams. The accelerometer sensors, strain sensors, hammer device are used to induce pitch and plunge motion. The particle photograph velocimetry is used to visualize the go with the drift. At 4, 6, 13Hz the pointy growth in significance is found, those values correspond to pitch, yaw and roll motion. For

airspeed 25.2 the acceleration values growth with time. The plunge damping issue will increase as airspeed will increase whereas the pitch damping issue decreases as the airspeed will increase. High amplitude LCO is found at dynamic stall. NACA 0018 is thick so the trailing area parting is envisioned to occur first. The essential regularity of the stall flutter oscillations residues unaffected through the stall tool and every other aerodynamic parameter. The flutter and stall flutter are associated through the important mode frequency i.e., pitch frequency in low static attitude mode [20]. The prior work should have been thoroughly examined in order to obtain a clear understanding of how to set up an experimental setup for inspection of the flutter response to the changes happening in the test section (as we are following an iterative method of inspection). Flutter analysis has become one of the vital responses. Moreover, this is a natural oscillation happening in the bodies of any structure in every human's working area. In this case it is aerospace in recent years, when it was previously designated for airplanes, autos, and other related fields... In 1899, the Wright brothers carried out the first experimental work of aero elasticity. Later, NASA conducted numerous experiments on flutter analysis. The Structural Dynamics Division at NASA Langley Research Center, known as the Benchmark Models Program, organized wind tunnel tests to reach their objective. The wing used in the test has the airfoil of NACA 0012 rectangular in shape when seen from top was fixed on the flexible two DOF mount system. There's no inertial connection in between two modes (Pitch/Plunge) because the system was developed that way [23]. The pitch and plunge motion parameters were determined using servo accelerometers. The research concentrated on conventional flutter, Stall flutter and plunge instability. Static ports arranged chord wise just on the wing were used to calculate pressure distributions. As per the findings, the traditional flutter boundary is distinguished by an unusual pattern of increasing dynamic pressure with increasing Mach number. A plunge instability domain was observed in the transonic regime, indicating that plunge mode caused flutter in that regime [24]. NASA conducted the research using the same benchmark model but with alternative airfoil wings. Where they tested airfoils named NACA 0012, NACA 64A010, and NACA SC (2)-0414. Classical flutter, transonic stall flutter, and plunge instability were all taken into account this time. The supercritical airfoil was the focus of most experiments. For

measuring forces, the experimental setup was not up to the mark and unproven. Dynamic movements were monitored using strain gauges and accelerometers installed on the model. For the data collecting system, benchmark active control technology was employed. Pressure transducers were carefully installed on wing models in a chord wise orientation at a certain span point [25]. Bendiksen and Saber investigate fluid–structure interaction problems that involve both structural and fluid nonlinearities. The exploration of nonlinear aero elastic stability constraints with wings with a high aspect ratio. Large deflections cause either aerodynamic and structural nonlinearities, which their finite element models account for. Svacek proposed a numerical simulation model of two-dimensional incompressible viscous flow coupling with a vibrating airfoil [26]. In the pitching direction, Zhen and Yang designed two-dimensional wings with cubic stiffness. The system's flutter velocity was then tested to Hopf bifurcation theory. The unpredictable reactions of an aero elastic system were estimated using a numerical integration method. Pang and Jinglong [18] analyzed the effect of wingtip devices on wing flutter using numerical models. Structural vibration has been determined by a computational structural dynamics (CSDs) solver only with geometric nonlinearity shown in the modeling, and unsteady aerodynamics were simulated using a computational fluid dynamics (CFDs) solver with the Euler equations presented as fluid governing equations [27]. Bendiksen and Saber investigate fluid–structure interaction problems that involve both structural and fluid nonlinearities. The exploration of nonlinear aero elastic stability constraints with wings with a high aspect ratio. Large deflections cause either aerodynamic and structural nonlinearities, which their finite element models account for. Svacek proposed a numerical simulation model of two-dimensional incompressible viscous flow coupling with a vibrating airfoil [26]. In the pitching direction, Zhen and Yang designed two-dimensional wings with cubic stiffness. The system's flutter velocity was then tested to Hopf bifurcation theory. The unpredictable reactions of an aero elastic system were estimated using a numerical integration method. Pang and Jinglong [18] analyzed the effect of wingtip devices on wing flutter using numerical models. Structural vibration has been determined by a computational structural dynamics (CSDs) solver only with geometric nonlinearity shown in the modeling, and unsteady aerodynamics were simulated using a

computational fluid dynamics (CFDs) solver with the Euler equations presented as fluid governing equations [27].

The interaction of CFD and CSD is examined, and the limit cycle oscillation response of a basic transport wing is estimated. By utilizing analytical and semi-analytical techniques, researchers have been attempting to forecast the frequency and amplitude of an airfoil's flutter oscillations for many years. The characterizing function approach, also known as harmonic balancing or linearization, is a common way for producing an analogous linear system that can subsequently be evaluated using classic linear aero elastic techniques. Chung proposed an incremental method and used it to solve free-play aero elastic problems. Haul and Chen investigated flutter using ANSYS software and the full-order and multimode methods [28]. Kargarnovin and Mamandi explored the effects of a sharp edged gust on an airfoil's reaction and flutter. Wang and Qiu¹¹ investigated the sensitivity of wing flutter speed to structural parameter uncertainty. An interval finite element model was developed and utilized to forecast the flutter critical wind speed range prediction. Bendiksen and Seber research fluid–structure interaction involves both structural and fluid nonlinearities. They looked at nonlinear aero elastic stability issues with high aspect ratio wings. Their finite element models account for both aerodynamic and structural nonlinearities caused by significant deflections. Svacek created a numerical simulation model of the interaction of two-dimensional incompressible viscous flow with a vibrating airfoil [29].

Aero elastic investigations of airfoil wings have been a fascinating component of the present study topic. Mazidi and Fazelzadeh recently showed the significance of wing sweep angle on the flutter limits of a wing/engine arrangement. A wing with an external storage has also been the subject of several studies as a common airplane layout. However, there is a scarcity of experimental research on these topics. Dowell and his research group have completed several tests on flutter experiments of a constant thickness cantilever delta wing with external storage. The air speed and flutter velocity are quite modest in the majority of these trials [30], Theodorsen was the first to discover the flutter phenomena in 1935. Since then, a large number of theoretical and experimental researches on this topic have been published, including Ashley and

Landahl, Bisplinghoff, and Ashley and Dowell. The desire for fast and nimble aircraft has surged recently. Active flutter suppression strategies are utilized to minimize flutter at low speeds and boost utter crucial speeds. To reduce flutter, Marretta and Marino presented a control flow based on a single input-single output controller. Lee investigated flutter as well as the open and closed-loop responses of a wing flap system employing sliding mode control [31].

In low subsonic flow, Dardel and Bakhtiari-Nejad proposed and included a static output feedback control for aero elastic management of a cantilevered rectangular wing. In a lightweight and low aspect ratio rectangle shaped nonlinear structural wing, they developed a control to extend the flutter boundary and suppress limit cycle oscillation. Analytical and semi-analytical methodologies have been used to predict the frequency and amplitude of flutter oscillations through an airfoil for many years [32]. This paper focuses on the creation of a numerical tool for aircraft wing fluid-structure interaction (FSI) calculations, in which the exterior airflow and interior structure interact, as well as wind tunnel testing of two half wing prototypes to effectively evaluate the numerical tool's accuracy. For the aerodynamic study, a panel approach was used, and for the structural analysis, a finite-element model with equivalent beam elements was used, both written in the MATLAB programming language. Area, airfoil cross-section shape, aspect ratio, taper ratio, sweep angle, and dihedral angle were used to parameterize the wing design [33].

CHAPTER-III

METHODOLOGY

Computational:

As the concern of this have a look at is to apprehend the flutter behaviour of an airfoil, computational fluid dynamics utility is used for evaluation. NACA 5 digit collection airfoils have been decided on in this kind of manner that the placement of camber movements from main area to trailing area in phrases of the share of the chord in every airfoil. The airfoil may be very finely meshed the use of triangles. Once the meshing is satisfactory, the mesh is imported for glide evaluation, wherein the pitch and plunge are studied one after the other at velocities of 60, 80, 100, 120, 140, 160, 180, 190, 195, and 200 meters per second.. Six diploma of freedom evaluation is used to present the enter parameters which include mass of the airfoil (m), spring stiffness in plunge movement (K_h), spring stiffness in pitch movement (K_α), mass second of inertia approximately aid point (I_α), function of middle of stress of aerofoil (X_{cp}), function of middle of mass (X_{cm}). These values have been stimulated from the observations of Davinder Rana et al [16]. Dynamic mesh is used for this evaluation because the frame wishes to react and displace primarily based totally at the reactions acquired from the air glide, wherein the dynamic mesh settings like spring element consistent, diffusion element and scaling element have been exact. The wing is dealt with as inflexible frame because it ought to now no longer deform, and its environment have been additionally dealt with as inflexible however as passive.

The whole outside a part of the surrounds could be set as a deforming mesh as this a part of the mesh has to deal with the deformation of the mesh resulting from the motion of the wing. Inspiring from the paintings of Davinder Rana et al [16], wherein they analysed the aerofoil for the variant in aerodynamic elevate that is primarily based

totally at the motion of the airfoil obliging to the given parameters of spring and so forth after which calculated the pitching and plunging displacement of the airfoil. In these findings the equal type of evaluation is performed, however the pitching and plunging of airfoil is exact with inside the dynamic mesh segment itself which offers us the liberty to have a look at the variant with inside the aerodynamic elevate. Based at the variant of the aerodynamic elevate alongside the time period, if the fluctuations of the aerodynamic elevate damps alongside the time it is able to be understood that the wing is getting stabilized, if the fluctuations are consistent over the time, it is able to be understood that frame is oscillating however isn't always fluttering, with inside the equal manner if the versions of the aerodynamic elevate is visible to boom with time it is able to be understood that the frame is fluttering. The airfoils have been restrained to transport handiest among superb perspective of assault of 10 deg to terrible perspective of assault of 10 deg and with inside the equal manner the airfoils have been restrained to a superb upward movement of 0.5 meters and to a downward movement of 0.5 meters. The middle of mass of the airfoil turned into constant at $c/4$ and the middle of flexural axis turned into constant ahead of the middle of mass at a distance of 0.15 m from the main fringe of the airfoil. Dynamic mesh turned into carried out and smoothing, layering and remeshing alternatives have been used to create the mesh in an effort to serve the cause. For the sake of pitching, one diploma of freedom rotation turned into used wherein as for the cause of plunge or heave movement, one diploma of translation turned into decided on with the restrictions as said with inside the above paragraph.

Inertia Properties	$m=51.5 \text{ Kg}$, $I_{yy}= 2.275 \text{ Kg m}^2$, $X_0 = 0.4 \text{ m}$, $X_{cm} = 0.4429 \text{ m}$, $X_A = 0.0429 \text{ m}$
Stiffness properties	$K_h = 50828.463 \text{ N/m}$, $K_\alpha = 35923.241 \text{ Nm/rad}$

Table 1: Implicit stiffness and inertia characteristics

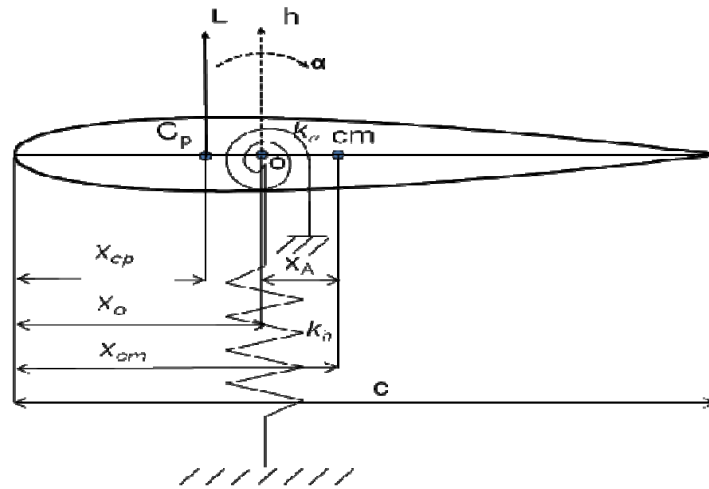


Figure 2: Aero foil structure

Experimental:

The experimental wing version turned into product of ribs fabricated from balsa timber and an Aluminium spar passing from the wingtip extending in addition off the hoop root such that it is able to be used to repair the wing version like a cantilever with inside the wind tunnel take a look at segment and this shape turned into protected with pores and skin and accelerometers are constant on the main and trailing edges of the wing tip. These accelerometers are related to an Arduino board so as to convert the vibrations inside the wing to the extrade in acceleration with recognize to time and could show in shape of graph with inside the utility interface this is hooked up with inside the computer.

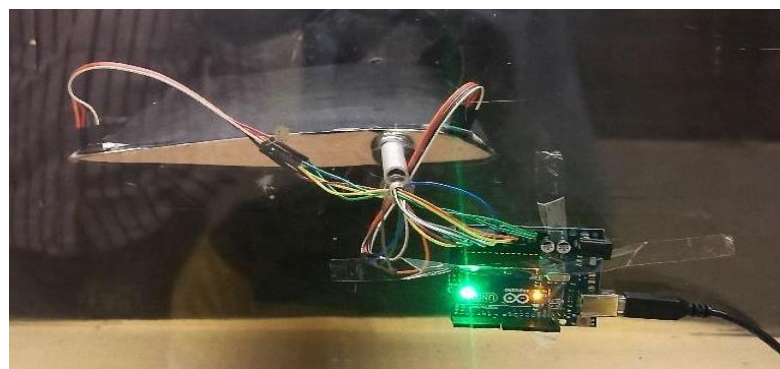


Figure 3 Wing installed with Arduino and accelerometers.

A small code is needed to be hooked up onto the Arduino board previous to this. The wing is constant with the assist of an aluminium spar like a cantilever beam and is to begin with constant at a 0° perspective of assault and is measured up to fifteen levels perspective of assault on all four wing models; then it's far examined on the inlet velocities beginning from 10 m/s to 40 m/s. the extrade in fee of acceleration with recognize to time are recorded. Recorded values are transformed to graphs the use of an easy MATLAB code in order that it would be smooth to research and apprehend the collective conduct of the wing. Figure1 suggests the setup of the wing with accelerometers related on the main and trailing area at the wing tip and an Arduino board with inside the wind tunnel.

Fabrication of the wing models

- a) To begin the construction process, we must first create a design layout using designing software and used those CAD files to laser cut the ribs that are required to fabricate the wing model.
- b) The wing model is created with chord length is 240mm, and span of 450mm and aspect ratio is 1.875 to make it fit in the wind tunnel test section.
- c) We prepared the laser cutting files to make 4 ribs for the wing models and then used a laser cutting tool to cut them out. The material used to make these ribs is 8mm thick balsa wood.
- d) A 6mm thick aluminium rods were used as spars that go into the wings and reinforce the structure.
- e) Monocot is used as the skin of these wing models which makes the surface of these models lighter and smoother.
- f) This has been done so that the wing model can be mounted in the wind tunnel like a cantilever beam that resembles the real time wing fixture.

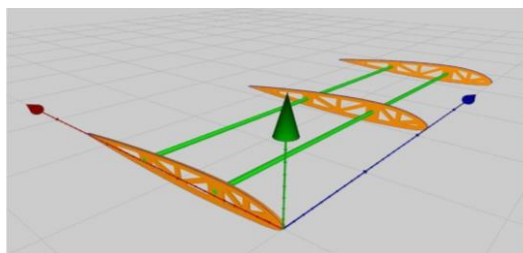


Figure 4. CAD file.



Figure 5. Ribs laser cutting.

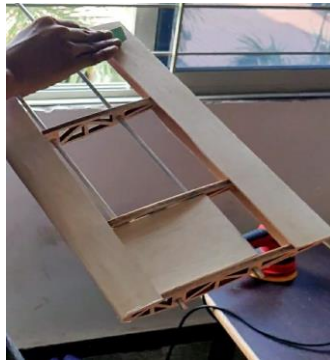


Figure 6. Ribs and spars after laser cutting.

Wind Tunnel Test Section

Coordinate system

- The x-axis is positive in the opposite direction of flow on the model.
- The y-axis is positive in the starboard side of the model in the wind tunnel test section.
- The z-axis is positive in the vertically upward direction of the model.
- For performing this analysis, a subsonic wind tunnel facility at institute of Aeronautical engineering was used.
- The wind tunnel has a test section of dimensions of 600mm X 600mm X 2000mm



Figure 7. low speed wind tunnel.

Arduino UNO Setup:

Accelerometer

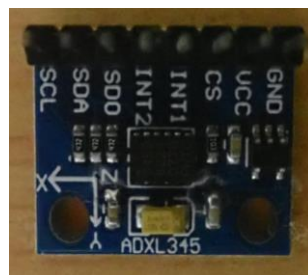
In this experiment we used the ADXL345 accelerometer sensor. It is a package of 3-axis acceleration measurement systems all in a single piece. It has a measurement range of $\pm 16g$ minimum. The ADXL345 uses a single structure for sensing the X, Y and Z axis.

Coordinate system

- a) The x-axis of the accelerometer is positive in the opposite direction of flow on the accelerometer.
- b) The y-axis is positive in the starboard side of the accelerometer which is attached to the wing model and placed in the wind tunnel test section.
- c) The z-axis is positive in the vertically upward direction of the accelerometer.

Arduino UNO

- a) Arduino uno board is the device used to transmit the code to the accelerometer where the device helps the sensor to obtain the acceleration in the x,y and z plane along with timestamp.



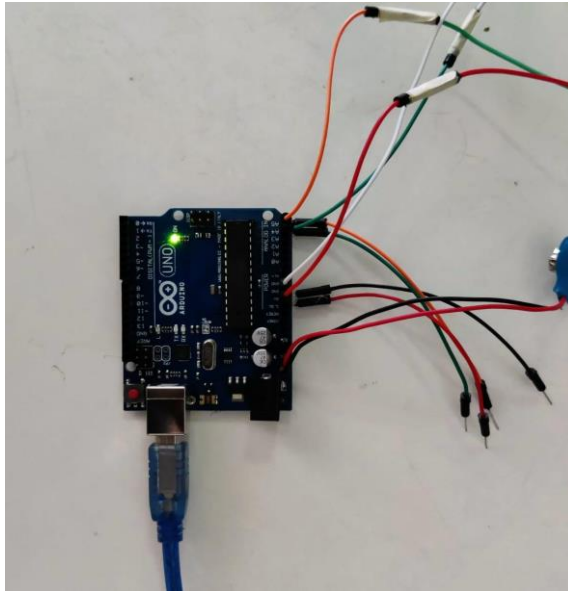


Figure 8. Arduino uno board and setup that was used for the experiment



Figure 9. Arduino setup with wing mounted in a wind tunnel.

CHAPTER IV

RESULTS & DISCUSSION

Computational:

Four special airfoils had been analysed below identical houses and situations to examine the behaviour of pitch and plunge and to describe the impact of camber over those motions. From the figures attached under we are able to see that the movement of the airfoil at decrease inlet speeds of 60 m/s is getting stabilized through the years with small preliminary disturbances, whilst the inlet velocity is various to one hundred sixty m/s it's miles found that the airfoil has regular motion alongside the time and is visible to have regular in addition to controlled movement each in pitch in addition to in plunge and at velocities of 195 m/s the airfoil appear to risky oscillations in pitching motion in which as in plunge movement, those airfoils appear to oscillate with greater frequency than at decrease inlet velocities. Negative lift is produced at higher negative angles of attack because the pressure distribution reverses, with higher pressure on the upper surface and lower pressure on the lower surface. This occurs when the angle of attack is below the zero-lift angle, causing the airfoil to generate a downward force.

We think that the camber movements from the main aspect toward the trailing aspect for the airfoils 21012, 22012, 23012, 24012 as the chord duration became maintained regular for all of the airfoils. By gazing the C_l plot of 21012 below pitching movement at low velocities of 60 m/s the airfoil appears to oscillate with inside the beginning and became stabilized soon, and on the velocities extra than one hundred sixty m/s the airfoil appears to oscillate out of control for few seconds after which became stabilized over the time and at velocities attaining two hundred m/s, the wing became oscillating continuously over a time frame and then began out to oscillate in out of control movement. Coming to the plunging movement, airfoil stabilizes with in a brief time frame at decrease velocities of 60 m/s and motions with lesser frequencies of better deflections at velocity of one hundred sixty m/s and sooner or later motions that have a clean smaller segment angles at better air inlet velocities of 195 m/s. And a comparable form of behavior may be found from reading the outcomes of NACA

22012, NACA 23012 and NACA 24012 airfoil sections. This will conclude the computational analysis for flutter in terms of the varying C_l with time in both pitch and plunge directions, then we move to the experimental analysis of the wing with help of wind tunnel and accelerometers.

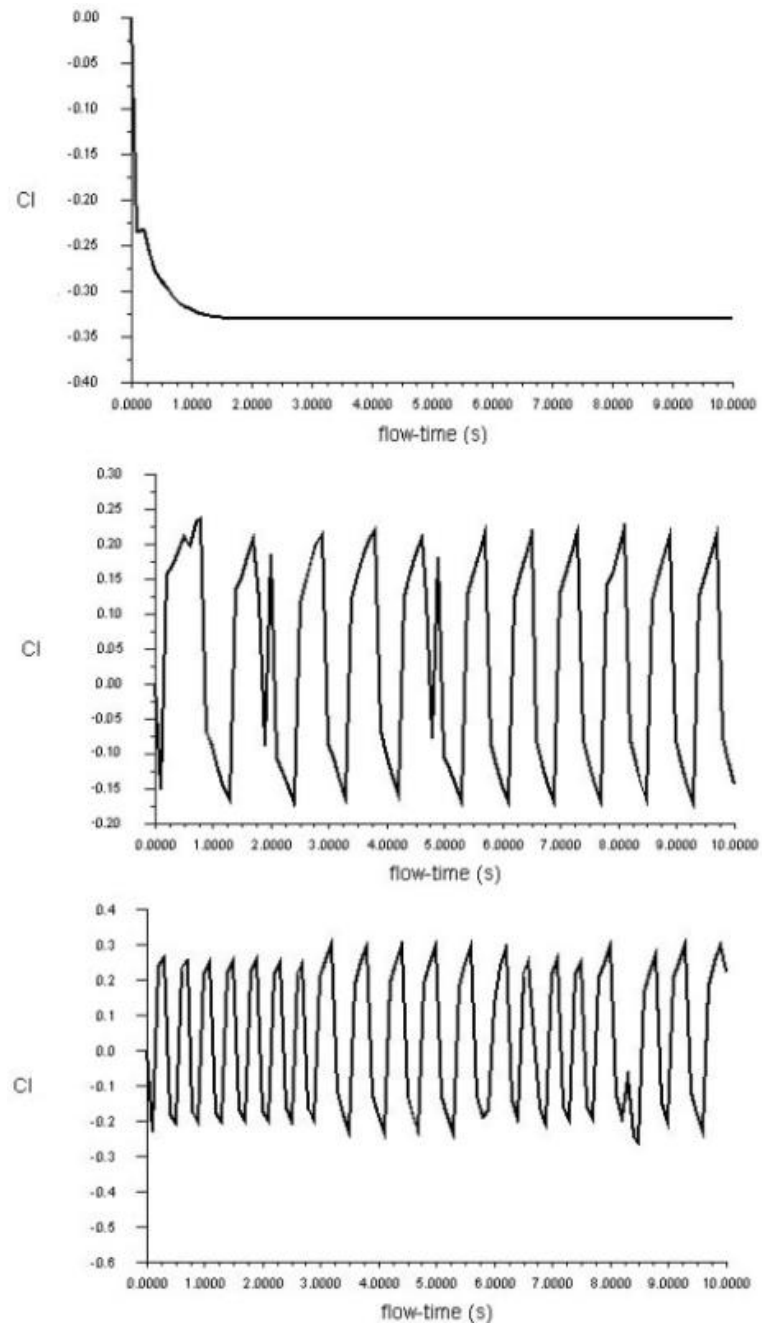


Figure 10. C_l versus α graph demonstrating the pitching motion of the 21012 airfoil.

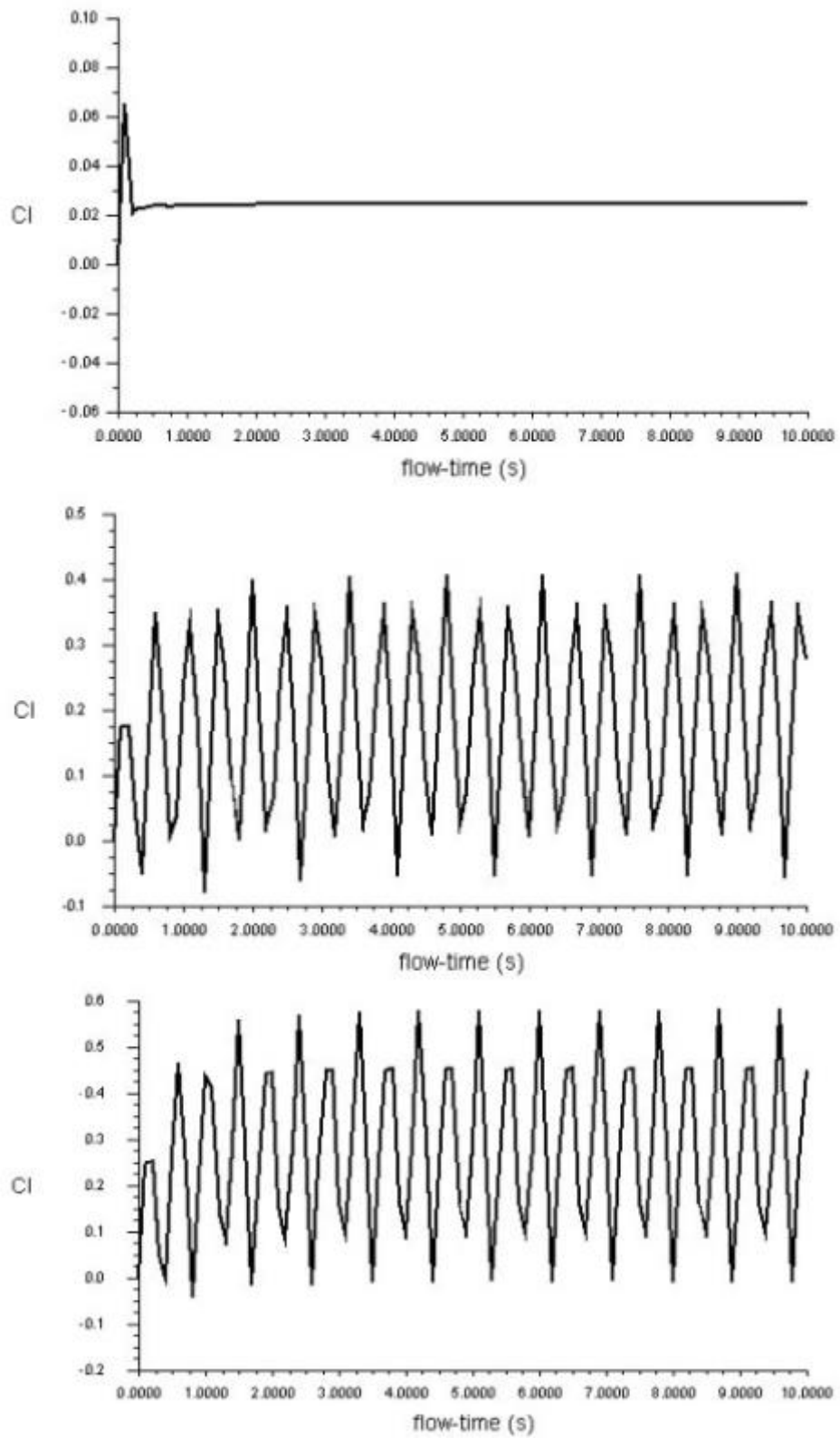


Figure 11.Cl versus alpha graph demonstrating the heave motion of the 21012 airfoil.

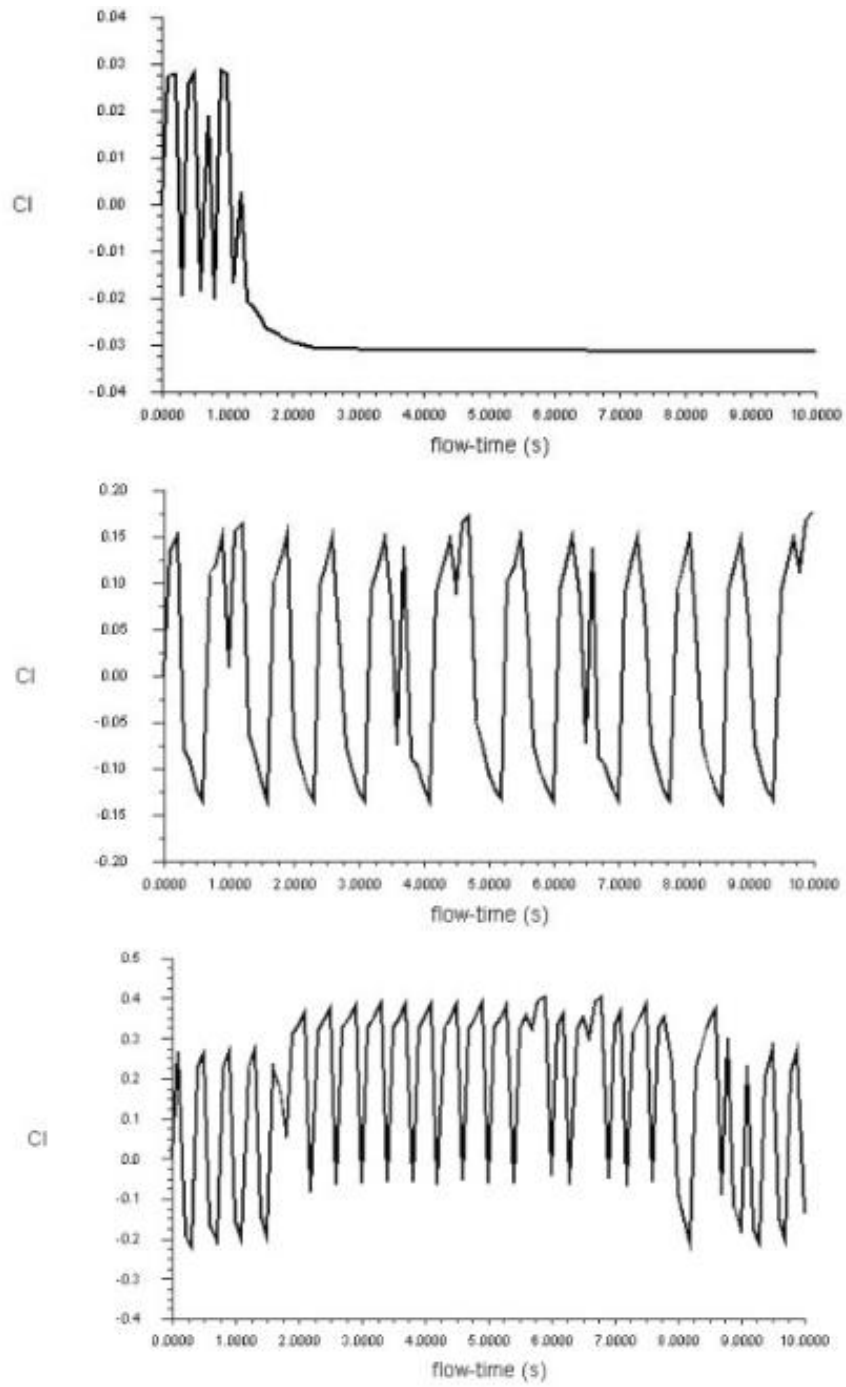


Figure 12. C_l versus α graph demonstrating the pitching motion of the 22012 airfoil.

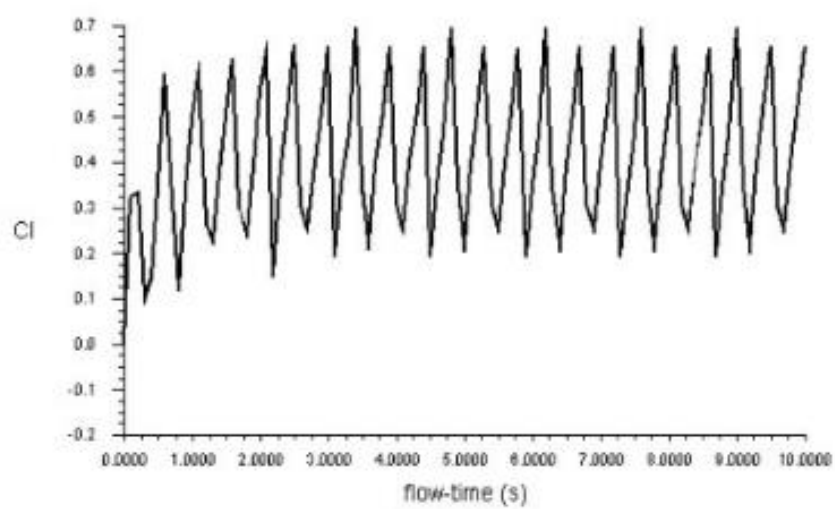
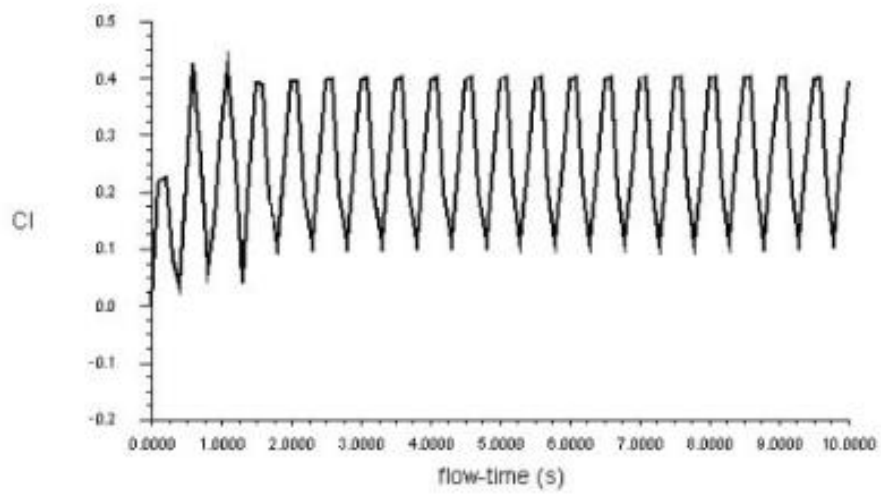
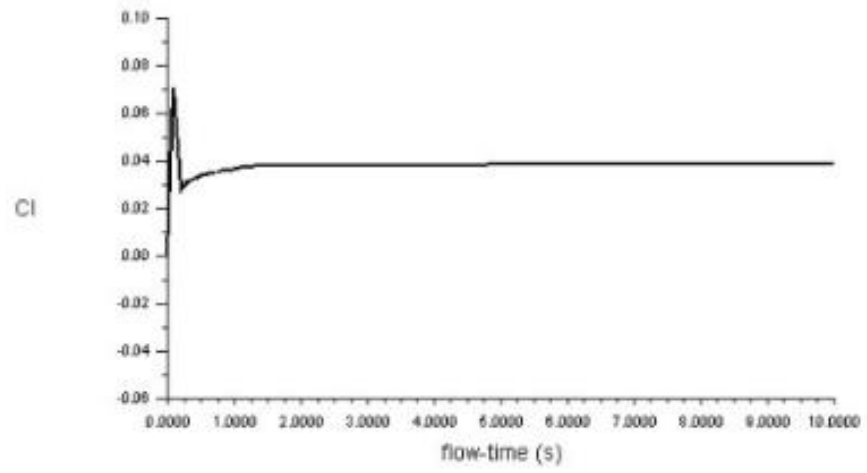


Figure 13. Cl versus alpha graph demonstrating the heave motion of the 22012 airfoil.

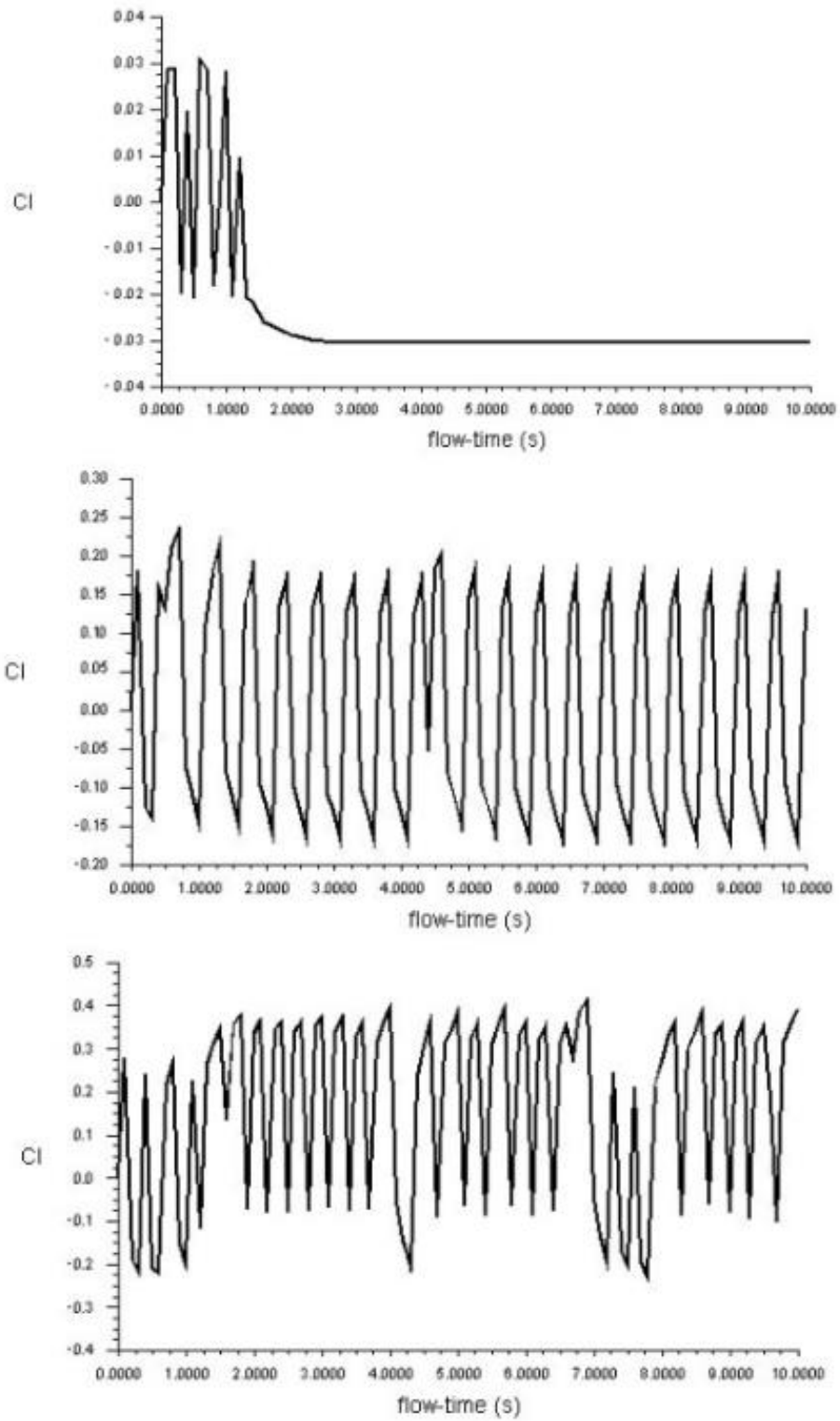


Figure 14. Cl versus alpha graph demonstrating the pitching motion of the 23012 airfoil.

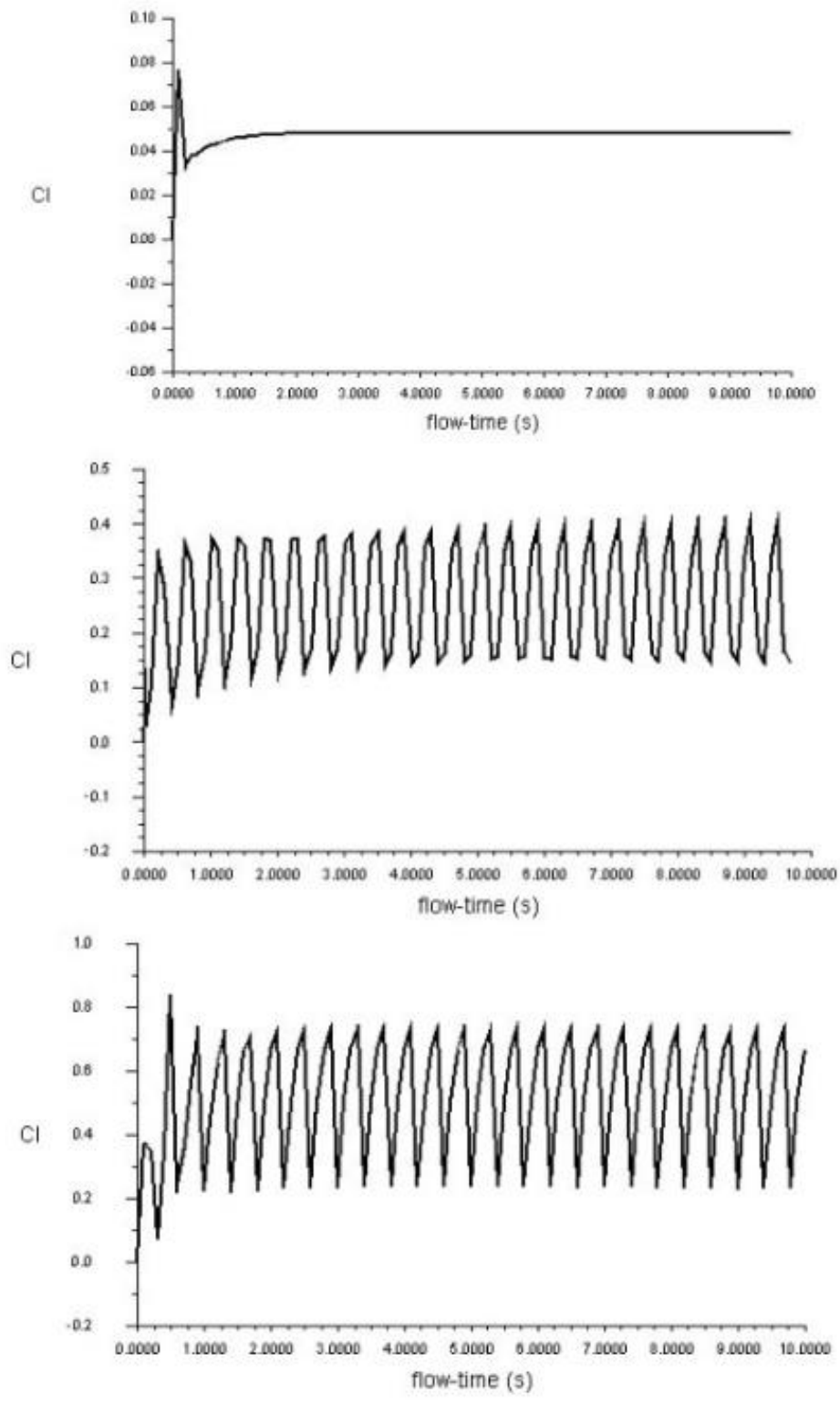


Figure 15. Cl versus alpha graph demonstrating the heave motion of the 23012 airfoil.

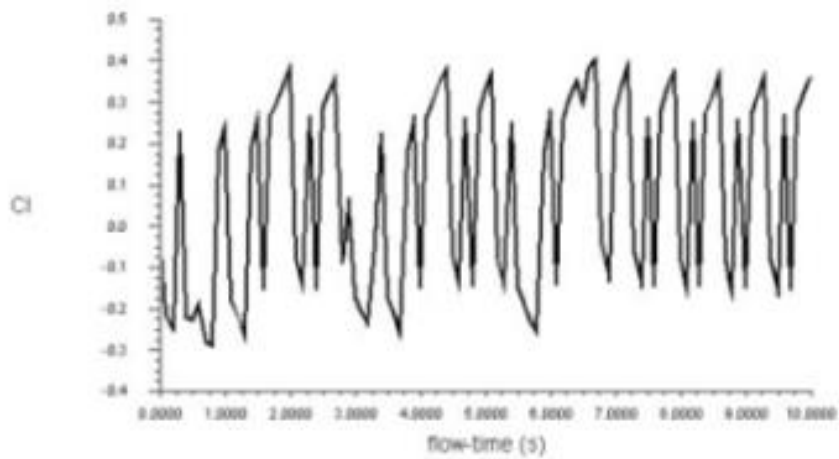
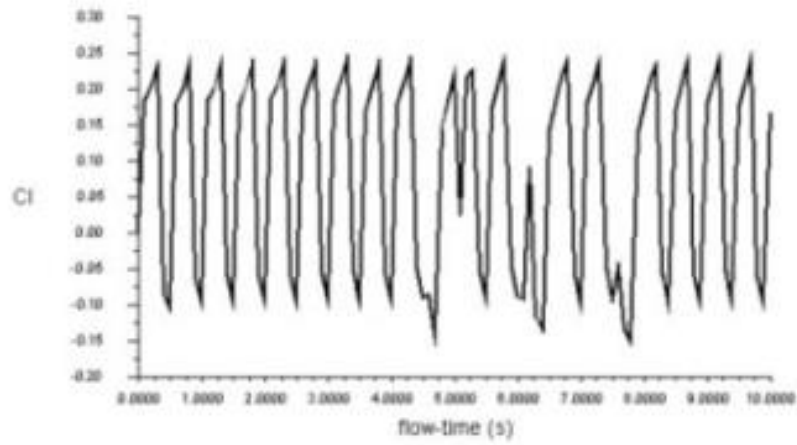
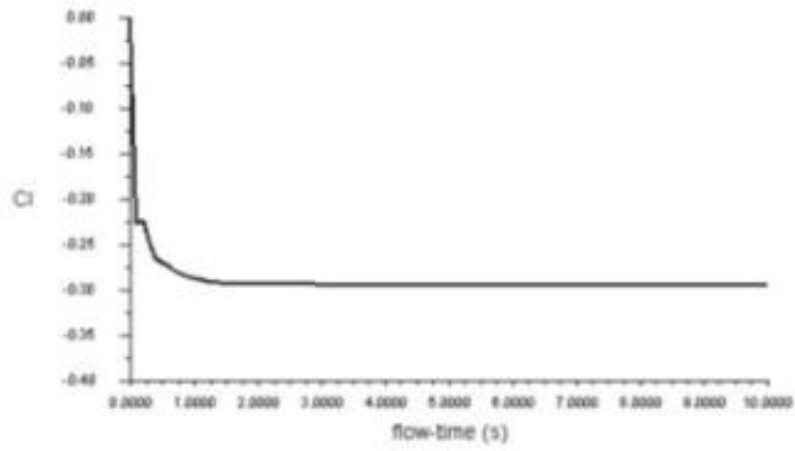


Figure 16. C_l versus α graph demonstrating the pitching motion of the 24012 airfoil.

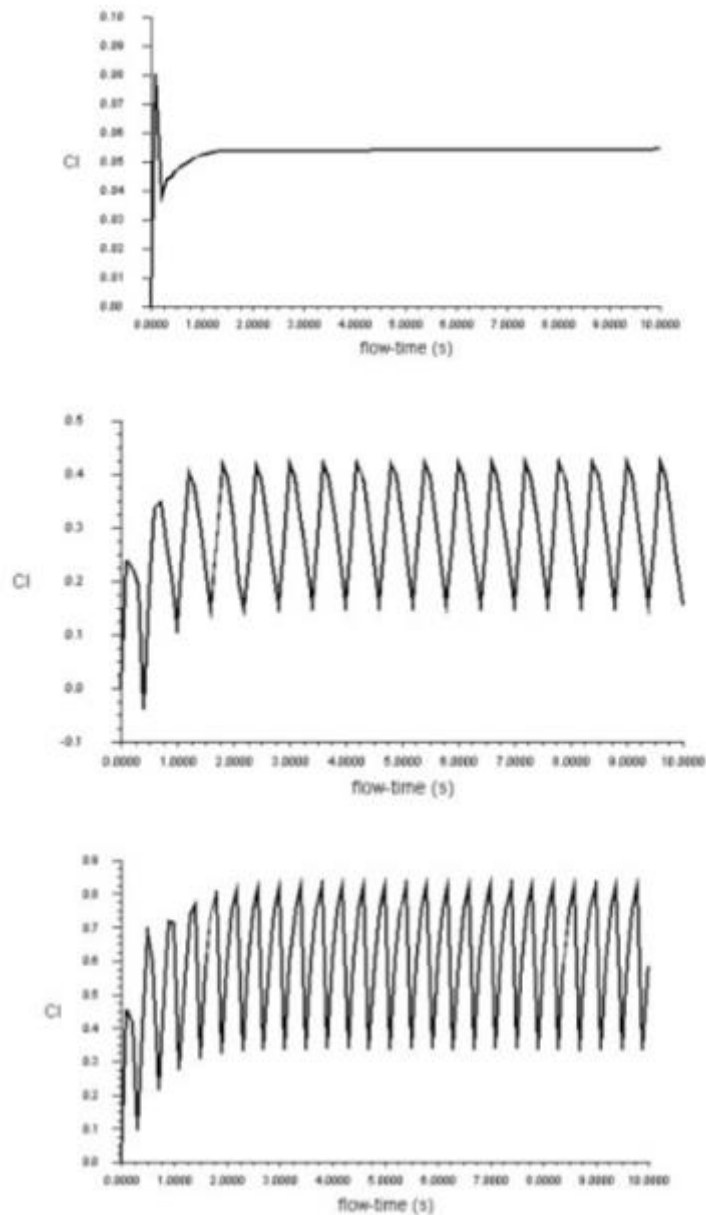


Figure 17. Cl versus alpha graph demonstrating the heave motion of the 24012 airfoil.

Experimental:

Considering the 21012 airfoil, wing begins off evolved to flutter at decrease velocities and at decrease attitude of assault however as the rate is accelerated, vibrations of decrease amplitude may be found. Flutter may be visible at 15 tiers of attitude of assault and at velocities which might be decrease than the flutter velocities of the identical wing at lesser attitude of assault of 10 tiers. The wing began out to

flutter absolutely at 15 tiers attitude of assault at 32.5 m/s air velocities and the vibrations have accelerated uncontrollably on the identical attitude of assault however at forty m/s. When the plots of 22012 airfoil are analyzed at an attitude of assault of 10 tiers and speed of forty m/s a totally few spikes of graphs of main and trailing aspect appear to coincide however whilst the attitude of assault is similarly accelerated to fifteen tiers at a speed of 25 m/s flutter appears to be induced. Wing appears to vibrate at better frequencies on the identical attitude of assault and velocities than that of 21012. Similarly, if 23012 wing is analyzed it's miles found at attitude of assault of 10 tiers and speed of forty m/s the wing main and trailing edges looked vibrate at comparable amplitude that is the identity factor that flutter is induced. At better velocities and better attitude of assault the amplitude and frequency of vibration have accelerated vigorously for the wing built out of 23012 airfoil. Finally, whilst 24012 is studied flutter appears to be induced at a decrease attitude of assault of 0 diploma and speed of forty m/s. Similarly, if the plots of 10 tiers attitude of assault and 32.5 m/s in addition to 10 tiers attitude of assault and forty m/s are as compared with the relaxation of the airfoils we are able to simply see that the wing began out to flutter at very early degrees than relaxation of the opposite 3 wings. When the velocities and attitude of assault accelerated simply obtrusive however the wing has vibrated critically and this could be concluded by gazing the extrude in values of acceleration with recognize to time of main and trailing edges.

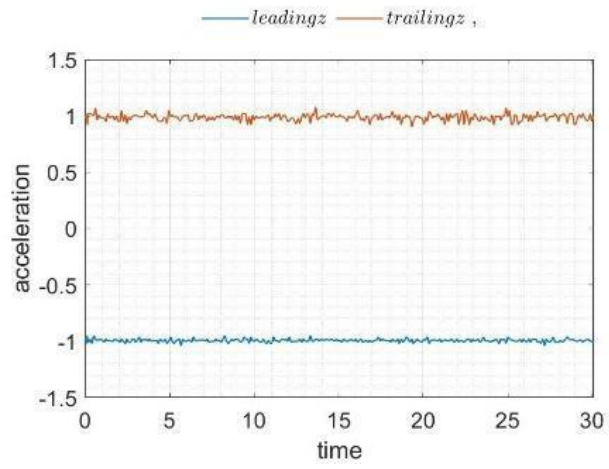


Figure 18. 21012 wing at AOA= 0° & inlet velocity = 10 m/s

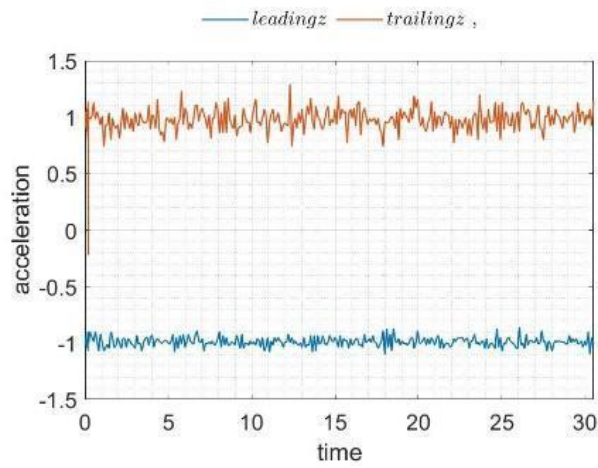


Figure 19. 21012 wing at AOA= 0° & inlet velocity = 17.5 m/s

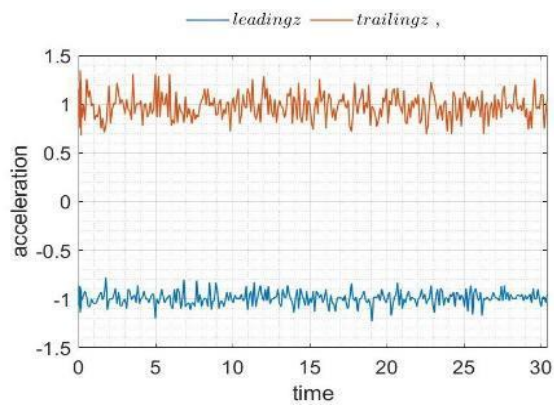


Figure 20. 21012 wing at AOA= 0° & inlet velocity = 25 m/s

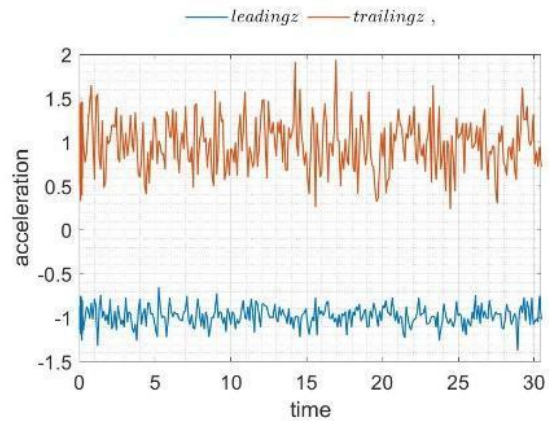


Figure 21. 21012 wing at AOA= 0° & inlet velocity = 40 m/s

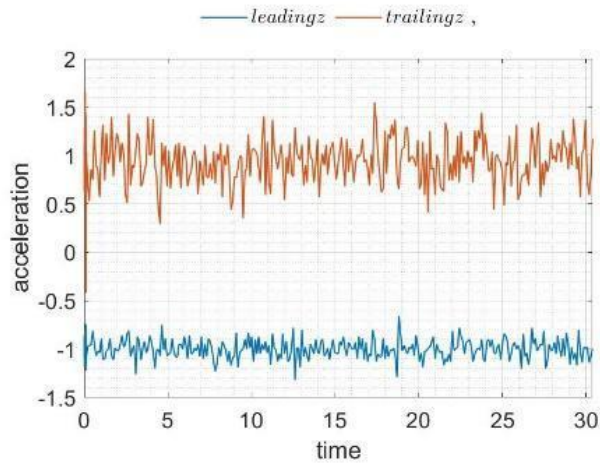


Figure 22. 21012 wing at AOA= 5° & inlet velocity = 32.5 m/s

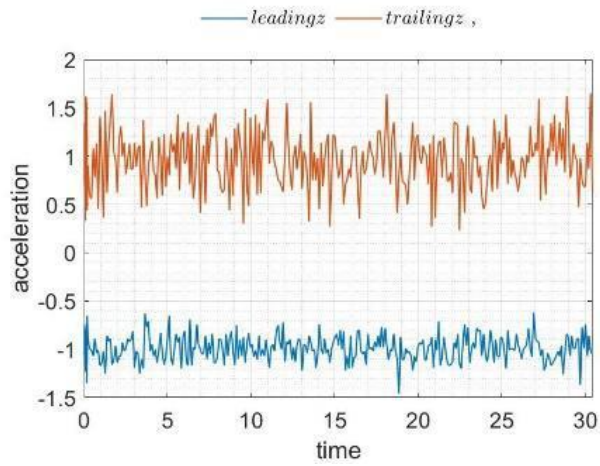


Figure 23. 21012 wing at AOA= 5° & inlet velocity = 40 m/s

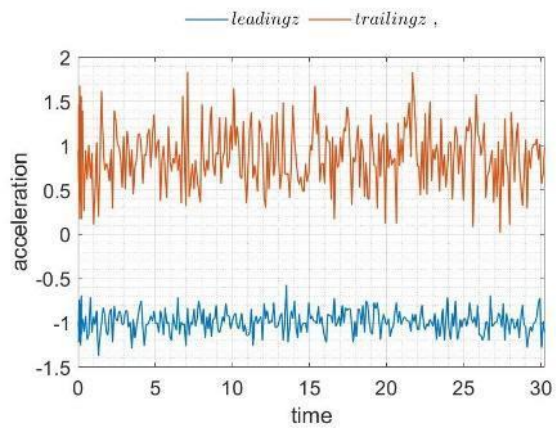


Figure 24. 21012 wing at AOA= 10° & inlet velocity = 40 m/s

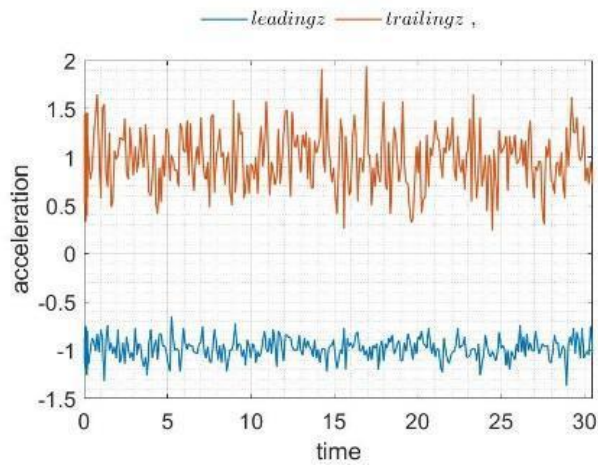


Figure 25. 21012 wing at AOA= 15° & inlet velocity = 10 m/s

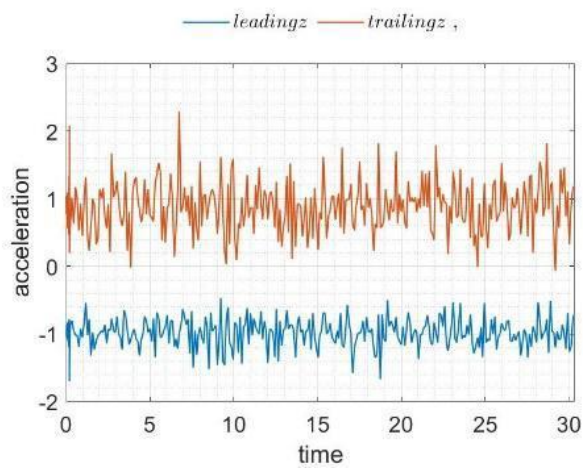


Figure 26. 21012 wing at AOA= 15° & inlet velocity = 17.5 m/s

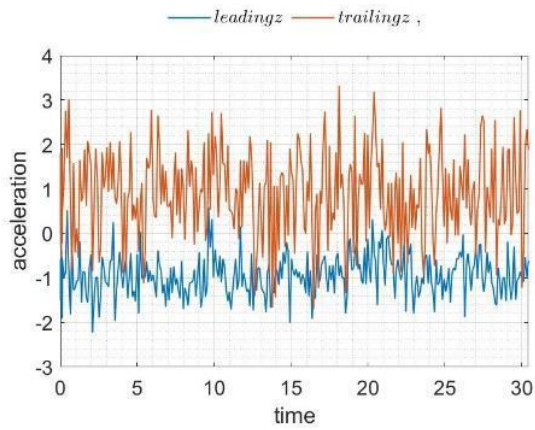


Figure 27. 21012 wing at AOA= 15° & inlet velocity = 25 m/s

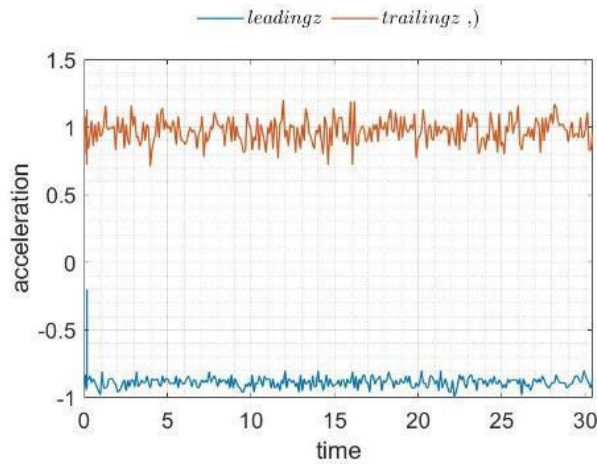


Figure 28. 21012 wing at AOA= 15° & inlet velocity = 32.5 m/s

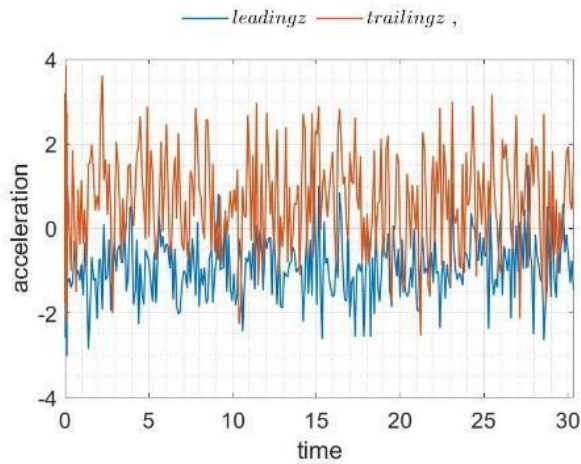


Figure 29. 21012 wing at AOA= 15° & inlet velocity = 40 m/s

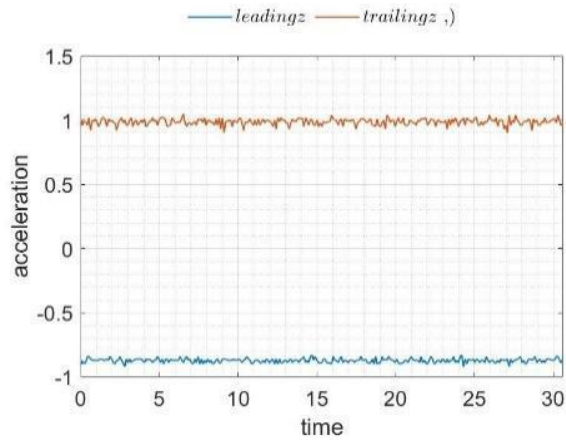


Figure 30. 22012 wing at AOA= 0° & inlet velocity = 10 m/s

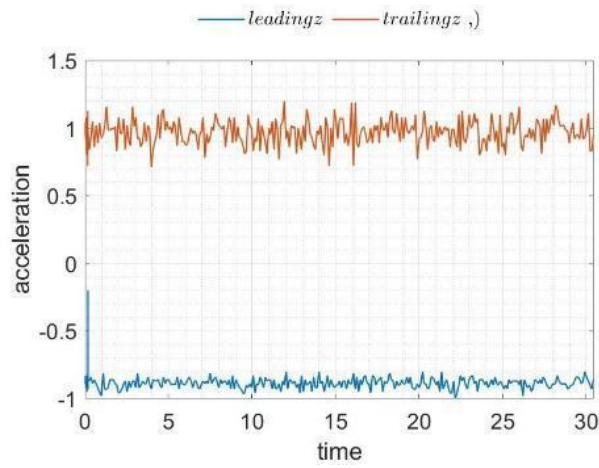


Figure 31. 22012 wing at AOA= 0° & inlet velocity = 17.5 m/s

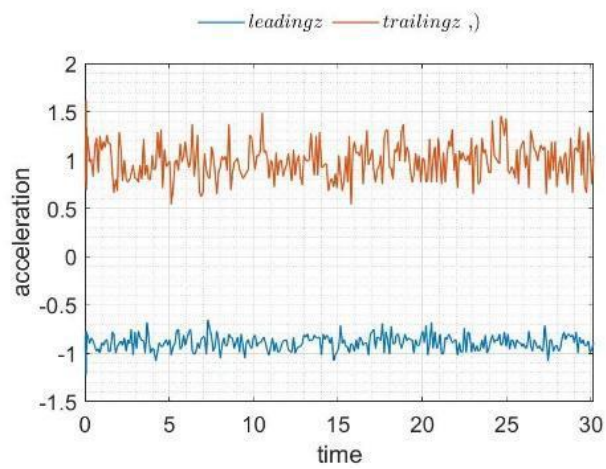


Figure 32. 22012 wing at AOA= 0° & inlet velocity = 25 m/s

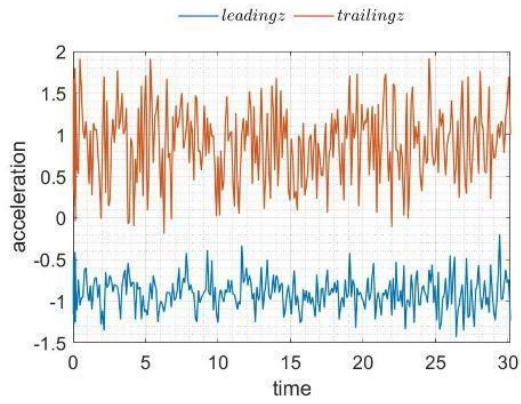


Figure 33. 22012 wing at AOA= 0° & inlet velocity = 40 m/s

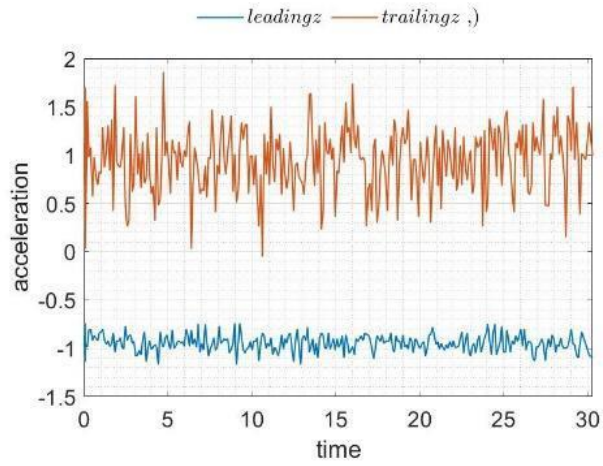


Figure 34. 22012 wing at AOA= 5° & inlet velocity = 32.5 m/s

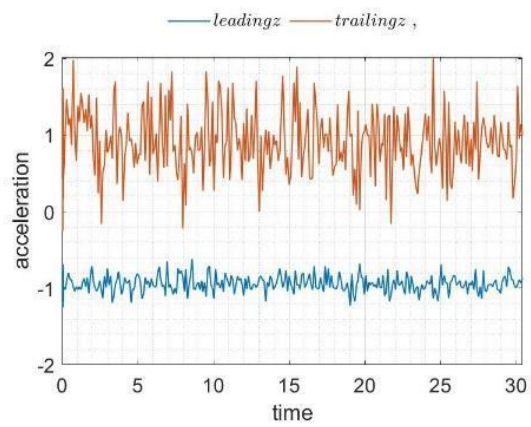


Figure 35. 22012 wing at AOA=5° & inlet velocity = 40 m/s

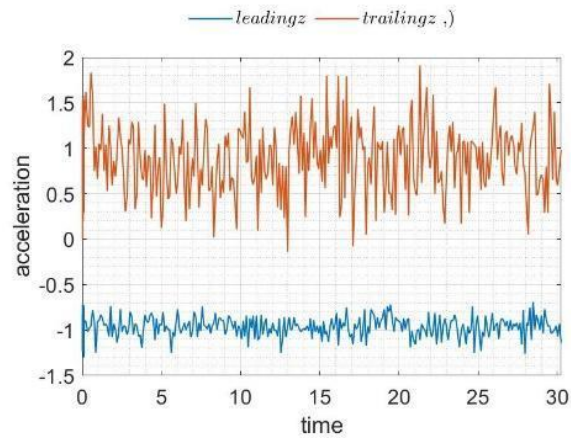


Figure 36. 22012 wing at AOA= 10° & inlet velocity = 32.5 m/s

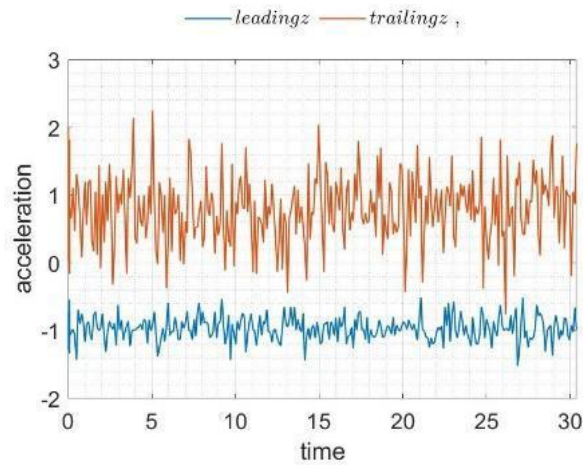


Figure 37. 22012 wing at AOA= 15° & inlet velocity = 40 m/s

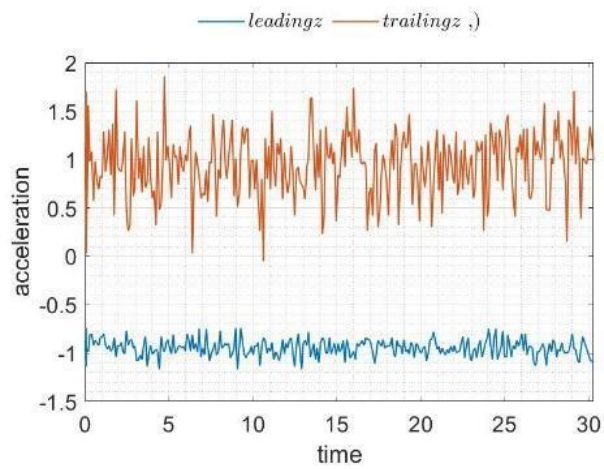


Figure 38. 22012 wing at AOA= 15° & inlet velocity = 17.5 m/s

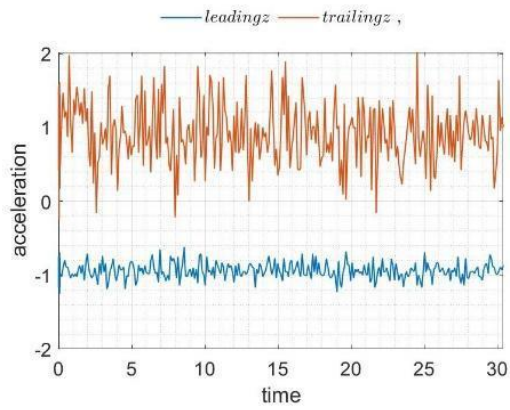


Figure 39. 22012 wing at AOA= 15° & inlet velocity = 25 m/s

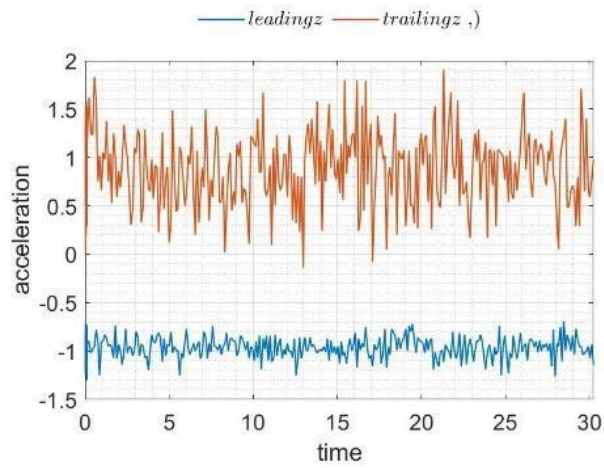


Figure 40. 22012 wing at AOA= 15° & inlet velocity = 32.5 m/s

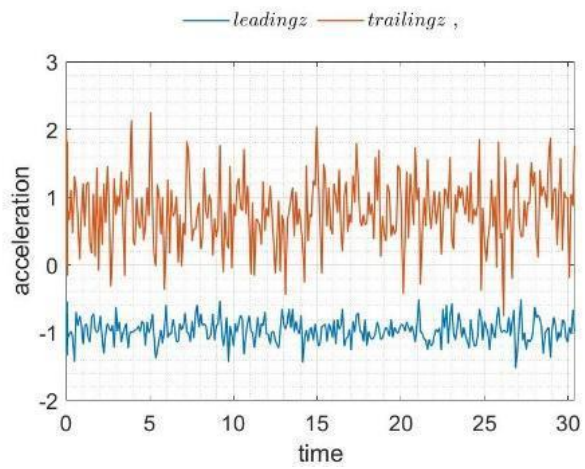


Figure 41. 22012 wing at AOA= 15° & inlet velocity = 40 m/s

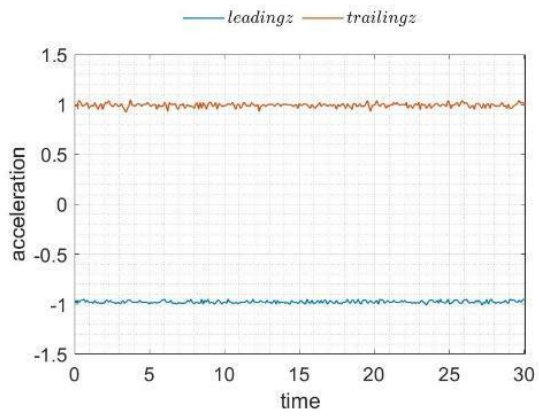


Figure 42. 23012 wing at AOA= 0° & inlet velocity= 10 m/s

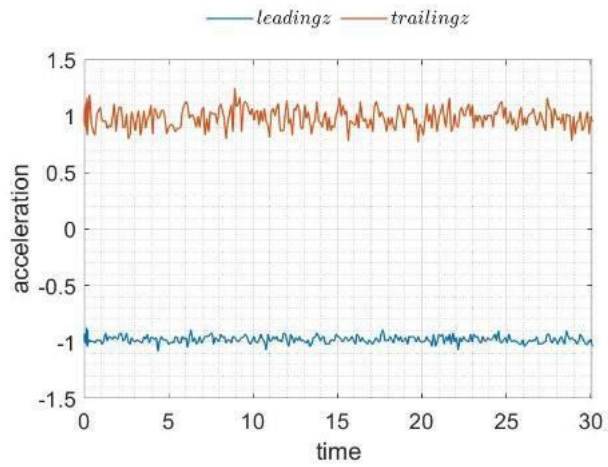


Figure 43. 23012 wing at AOA= 0° & inlet velocity = 17.5 m/s

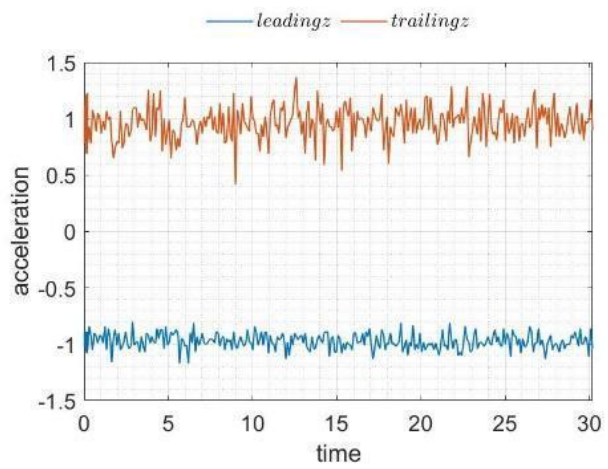


Figure 44. 23012 wing at AOA= 0° & inlet velocity = 25 m/s

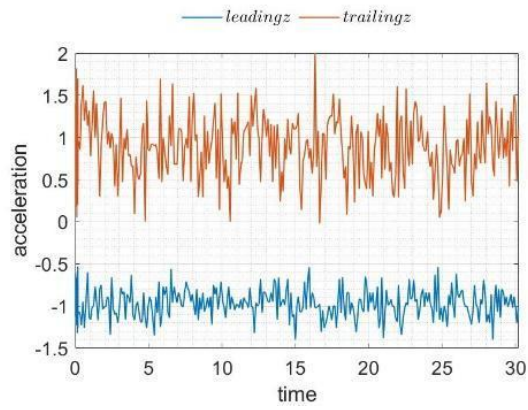


Figure 45. 23012 wing at AOA= 0° & inlet velocity = 40 m/s

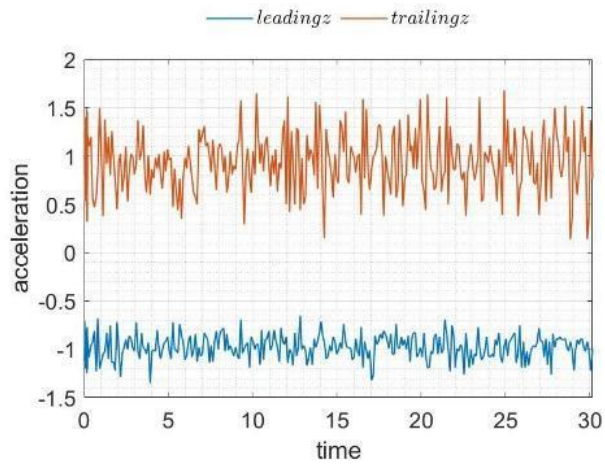


Figure 46. 23012 wing at AOA= 5° & inlet velocity = 32.5 m/s

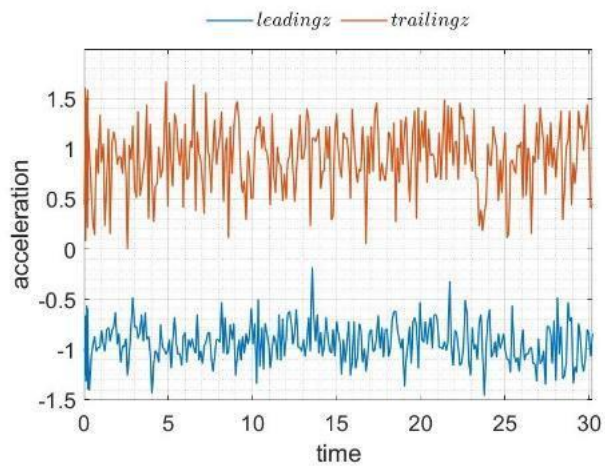


Figure 47. 23012 wing at AOA= 5° & inlet velocity = 40 m/s

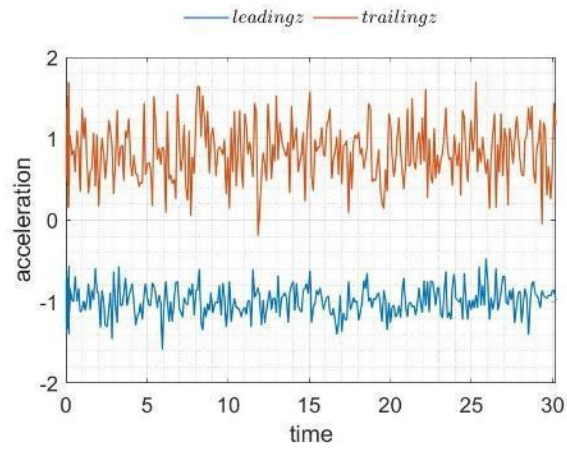


Figure 48. 23012 wing at AOA= 10° & inlet velocity = 32.5 m/s

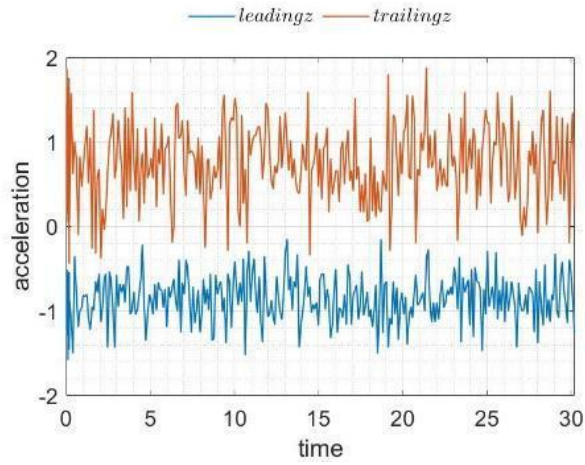


Figure 49. 23012 wing at AOA= 10° & inlet velocity = 40 m/s

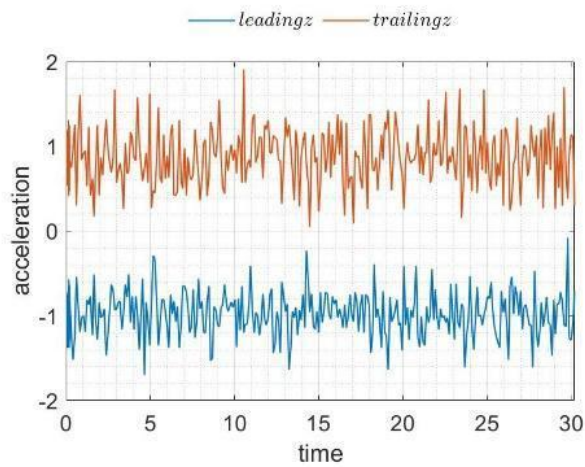


Figure 50. 23012 wing at AOA= 15° & inlet velocity = 17.5 m/s

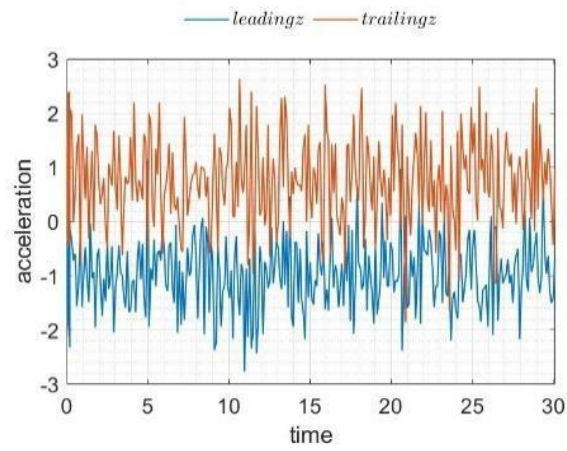


Figure 51. 23012 wing at AOA= 15° & inlet velocity = 25 m/s

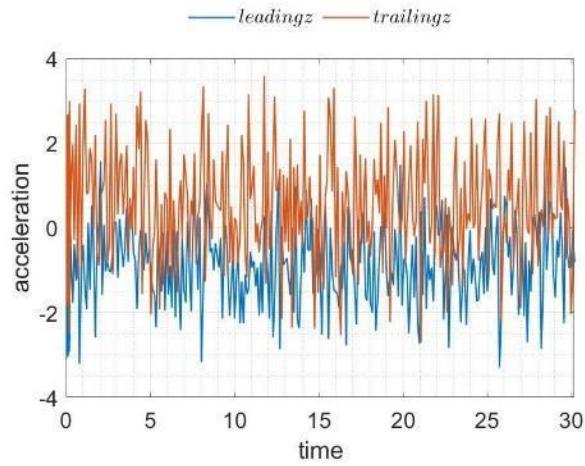


Figure 52. 23012 wing at AOA= 15° & inlet velocity = 25 m/s

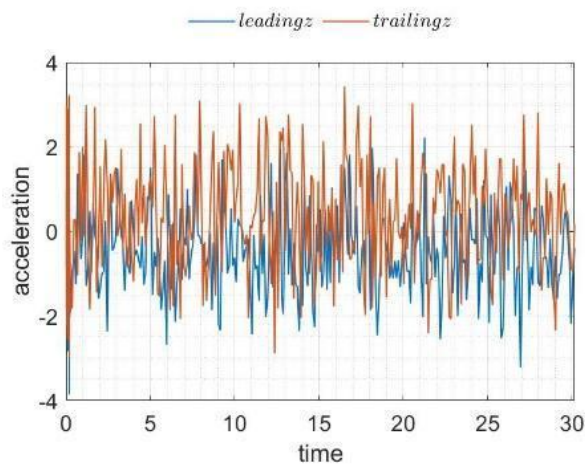


Figure 53. 23012 wing at AOA= 15° & inlet velocity = 40 m/s

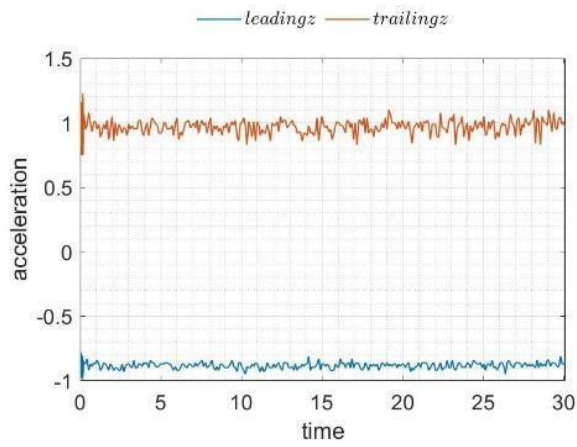


Figure 54. 24012 wing at AOA= 0° & inlet velocity = 10 m/s

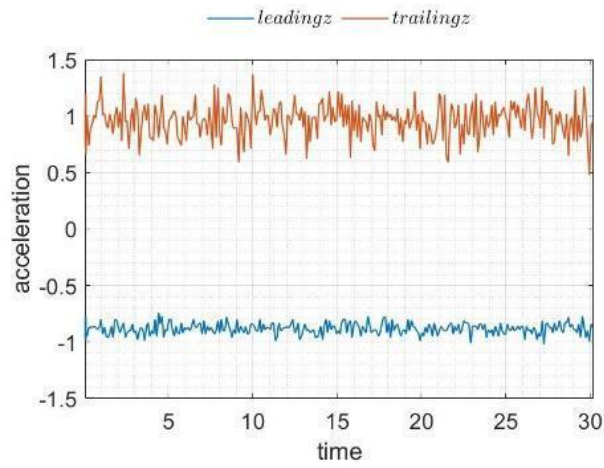


Figure 55. 24012 wing at AOA= 0° & inlet velocity = 17.5 m/s

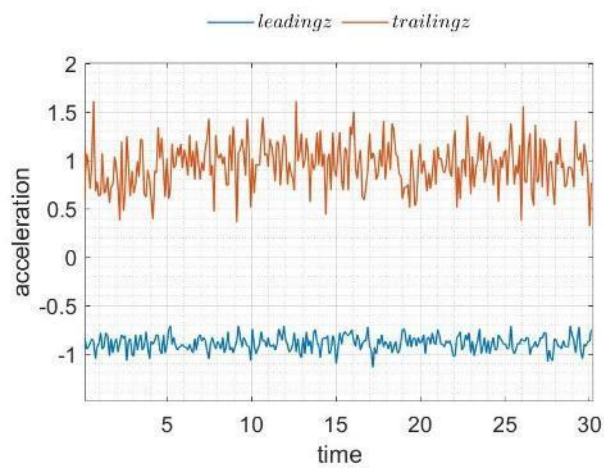


Figure 56. 24012 wing at AOA= 0° & inlet velocity = 25 m/s

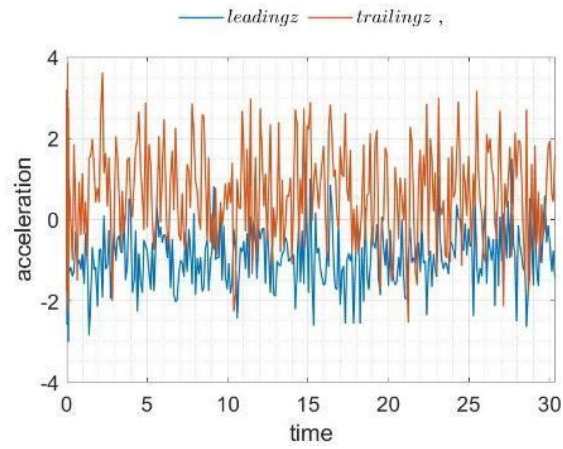


Figure 57. 24012 wing at AOA= 0° & inlet velocity = 40 m/s

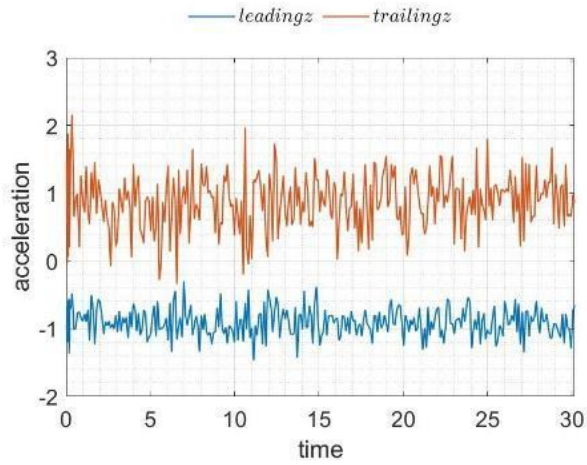


Figure 58. 24012 wing at AOA= 5° & inlet velocity = 32.5 m/s

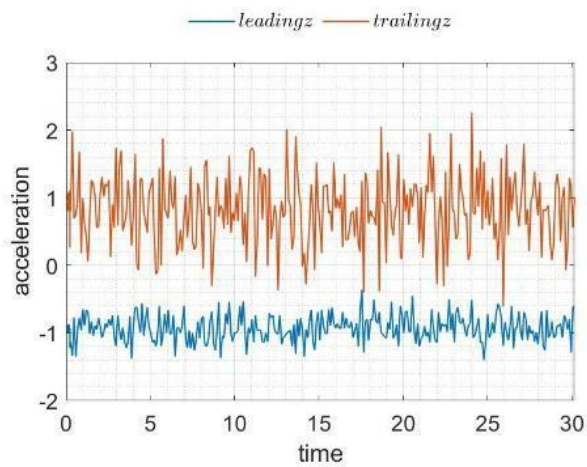


Figure 59. 24012 wing at AOA= 5° & inlet velocity = 40 m/s

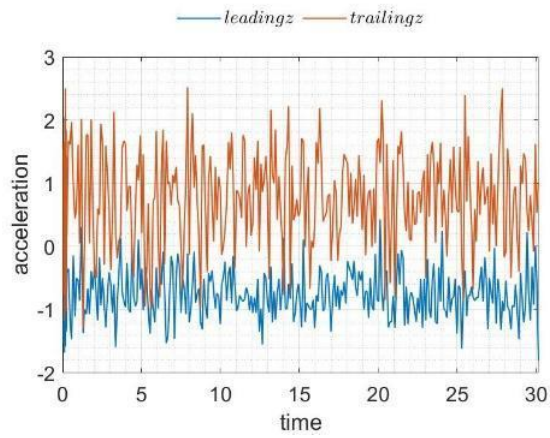


Figure 60. 24012 wing at AOA= 10° & inlet velocity = 32.5 m/s

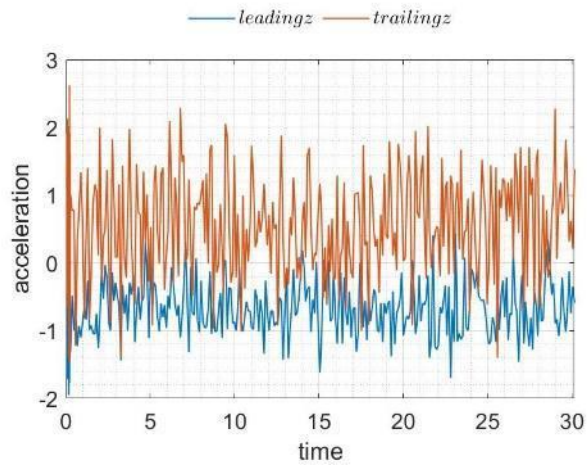


Figure 61. 24012 wing at AOA= 10° & inlet velocity = 40 m/s

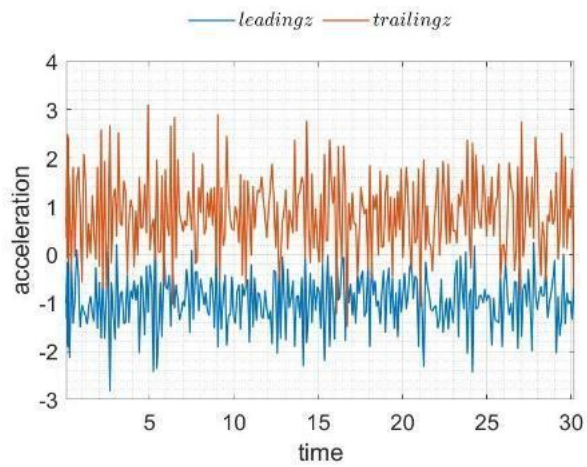


Figure 62. 24012 wing at AOA= 15° & inlet velocity = 17.5 m/s

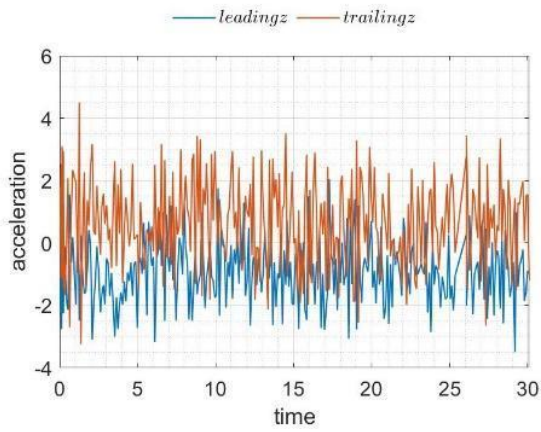


Figure 63. 24012 wing at AOA= 15° & inlet velocity = 25 m/s

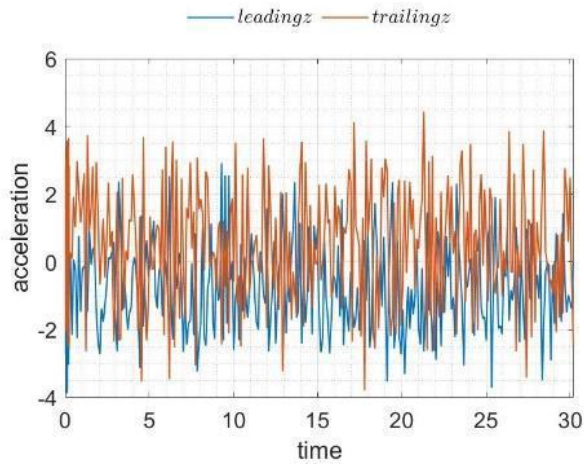


Figure 64. 24012 wing at AOA= 15° & inlet velocity = 32.5 m/s

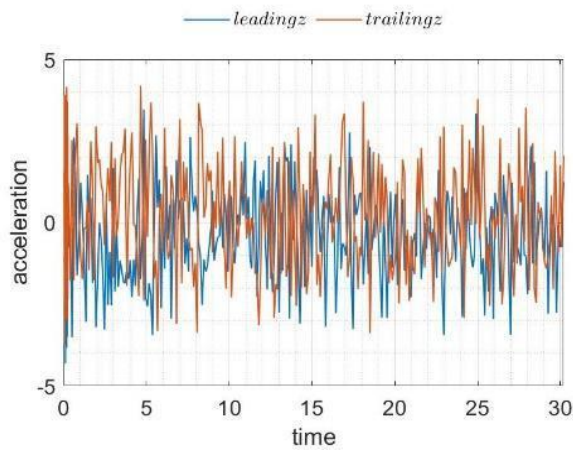


Figure 65. 24012 wing at AOA= 15° & inlet velocity = 40 m/s

Till now, NACA 21012, 22012, 23012, 24012 were studied, For understanding and validating the dependence of flutter on camber position, the airfoils 31015 and 34015 were selected for wind tunnel analysis using accelerometers. The primary reason for choosing these airfoils is their distinct differences in the position of maximum camber. Specifically, airfoil 31015 has its maximum camber located at 5% of the chord length, while airfoil 34015 has its maximum camber positioned at 20% of the chord length. This variation in the camber position is the only parameter altered in our wing model experiments.

Accelerometers were strategically placed at the leading and trailing edges of the wing, as well as at the tip of the wing. These sensors are connected to an Arduino board, which is programmed to measure and record acceleration data. The wing models were constructed with a chord length of 240 mm and a span of 450 mm. The structure of the wing is supported by an aluminum spar and ribs made from balsawood, with the entire assembly covered in a monocoque skin. The wing is mounted as a cantilever beam within the wind tunnel for testing. The variation of acceleration with time that was recorded using accelerometers was translated to frequency using FFT and the comparison plots were created.

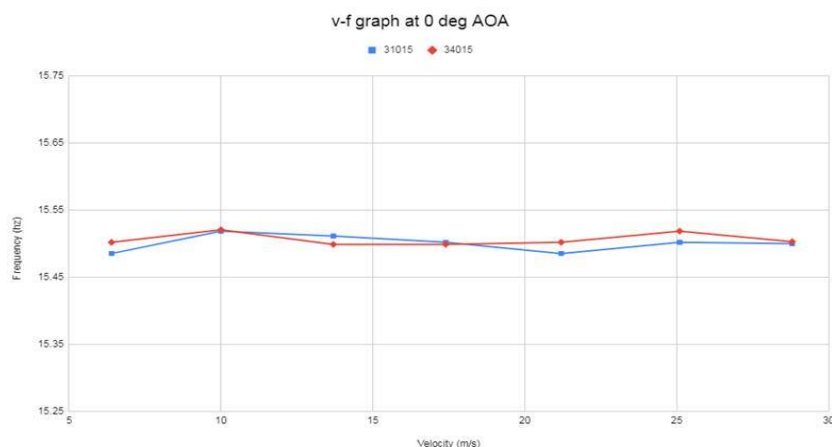


Figure 66. Comparison between v-f behavior of 31015 and 34015 airfoils at 0° angle of attack

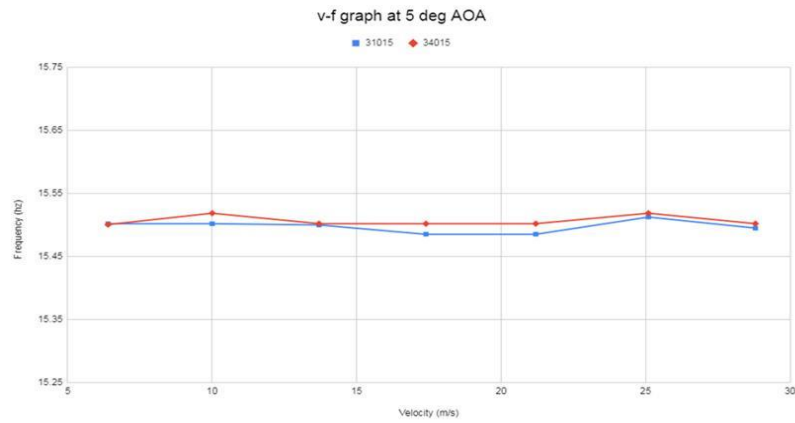


Figure 67. Comparison between v-f behavior of 31015 and 34015 airfoils at 5° angle of attack

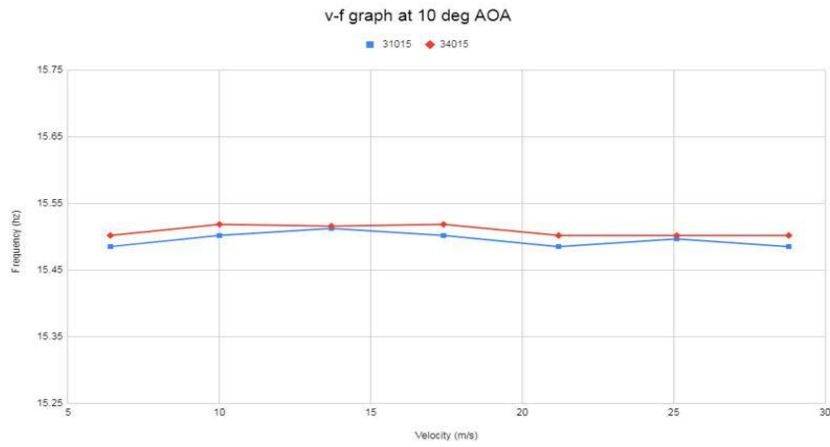


Figure 68. Comparison between v-f behavior of 31015 and 34015 airfoils at 10° angle of attack

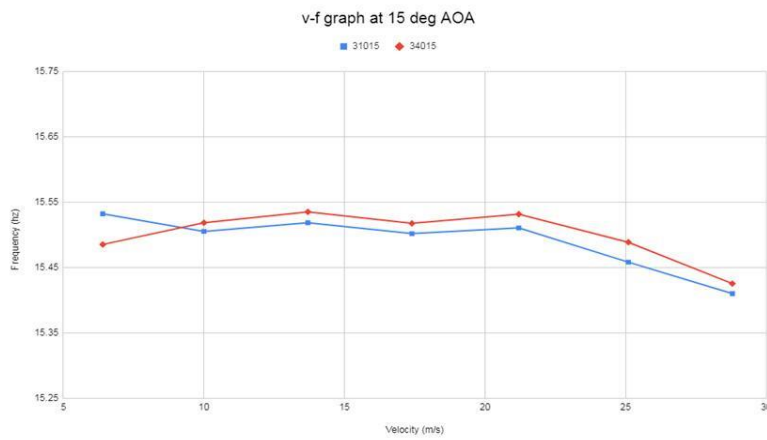


Figure 69. Comparison between v-f behavior of 31015 and 34015 airfoils at 15° angle of attack

CHAPTER- V

CONCLUSIONS

From diverse outputs that have been received after numerous computations, the results that portrayed a super alternate with inside the behaviour of the coefficient of lift have been analysed and from the graphs displayed, it's far surely obtrusive that the instability in pitching movement of the airfoil became greater as the placement of highest camber value movements towards the of flexural axis at the airfoil. When the plunging movement became determined for the version of coefficient of lift, there has been an unsteady and abnormal version determined with inside the values of coefficient of lift this may be visible with inside the Cl vs time plot of the 21012 airfoil, for this airfoil the vicinity of most camber is a far away than as compared to that of the opposite airfoils that are 22012, 23012 and 24012 as there may be no a good deal fluctuations to be visible with inside the graph of 21012 as compared to the rest. In the case of pitching motion, whilst each the pitching and plunging movement of the airfoil is mixed and determined, it's far surely understood that the airfoil is below flutter movement at the rate of 195 m/s as there has been a few regular fluctuations with inside the plunge movement of the airfoil, in which as an unsteady and unpredictable motion became determined with inside the pitching movement of the airfoil. Focusing at the impact of role of camber at the flutter phenomenon, because the vicinity of camber is shifting toward the middle of flexural axis it became surely determined that flutter became inevitable at the early time itself, this became surely obtrusive through gazing the pitching movement of 21012, 22012, 23012, 24012 airfoils.

Based at the air inlet pace at which flutter is induced and on the depth of the flutter at precise air speeds, it could be concluded from the above graphs that the flutter is induced at early airspeeds whilst the vicinity of most camber is toward the flexural axis, that's constant at 40 percentage of the wing chord. Flutter seems to set off at decreasing air velocities and primarily based totally at the closeness of the crests in the acceleration as opposed to time graphs, it could be surely understood that the flutter is

greater rigorous within the identical case. If the graphs of airfoil 21012 are studied, it could be visible that the flutter isn't very excessive at decrease air velocities, and even at better attitude of attacks, however if the plots of different airfoil are studied, it could be noticed that the early maximum flutter may be visible for 24012 airfoil or even the depth of the vibrations also are very excessive for the identical wing even though the simplest distinction among those wings is the vicinity of most camber. The similar behavior pattern could also be observed when further experiments were conducted on NACA 31015 and 34015 airfoils. Hence, from the above test and consequences, it could be understood that the vicinity of most camber impacts the flutter traits primarily based totally at the vicinity of flexural axis and the similar conclusions have been made with inside the preceding posted articles which have been primarily based totally on computational analysis (22).

1) REFERENCES:

1. Augustin Petre & Holt Ashley (1975). Drag effects on wing flutter. *AIAA Journal*. 1- 10.
2. Moses G. Farmer and Perry W (2012). Itanson. Comparison of supercritical and conventional wing Flutter characteristics. *AIAA Journal*. 608 – 614.
3. Bendiksen, Oddvar. (2011). Review of unsteady transonic aerodynamics: Theory and applications. *Progress in Aerospace Sciences*. 47. 135-167.
4. A. S. Mirabbashi, A. Mazidi, M. M. Jalili Analytical and experimental flutter analysis of a typical wing section carrying a flexibly mounted unbalanced engine. *International Journal of Structural Stability and Dynamics*. 2018.
5. Mazidi, Abbas & Fazelzadeh, S. (2013). Aero elastic Modeling and Flutter Prediction of Swept Wings Carrying Twin Powered Engines. *Journal of Aerospace Engineering*. 26. 586-593.
6. Gjerek, Bojan & Drazumeric, Radovan & Kosel, Franc. (2014). Flutter behavior of a flexible airfoil: Multiparameter experimental study. *Aerospace Science and Technology*. 36. 75-86.
7. Cui, Peng & Han, Jinglong. (2012). Prediction of flutter characteristics for a transport wing with wingtip devices. *Aerospace Science and Technology - AEROSP SCI TECHNOL*. 23.
8. Abbas, Mohammed & Yang, Zhichun & Gu, Yingsong & Wang, Wei & Safwat, Ehab. (2019). Active dynamic vibration absorber for flutter suppression. *Journal of Sound and Vibration*. 115110.
9. Li, Wencheng & Jin, Dongping. (2018). Flutter suppression and stability analysis for a variable-span wing via morphing technology. *Journal of Sound and Vibration*. 412. 410-423.
10. Garafolo, Nicholas & Mchugh, Garrett. (2017). Mitigation of flutter vibration using embedded shape memory alloys. *Journal of Fluids and Structures*. 76
11. Menon K, Katz. J and Mittal. R., "Computational Modeling and Analysis of Aero elastic Wing Flutter", *Fluid Dynamics Conference, AIAA AVIATION Forum*, 1-4, 2017.
12. Sasanapuri, Balasubramanyam & Zore, Krishna & Bish, Eric, "Aero elastic Simulations Using ANSYS Multiphysics Software", 58th, *AIAA/ASCE/AHS/ASC Structures, Structural Dynamics, and Materials Conference*. 1-5, 2017.
13. Chidambaranathan, Bibin & Selvaraj, Micheal & Sanju, Sanjukumar. Flutter Analysing Over an Aircraft Wing During Cruise Speed. *International Conference on Modelling Optimization and Computing*. 38. 1950-1961. 2012.

14. inproceedings Simulation OA, "Simulation of Aerodynamic Divergence and Flutter on Wind Turbines using ANSYS-CFX", D. Ramdenee and Sorin Ion Minea and A. Ilinca, 2012.
15. Kim, Dong-Hyun & LEE, IN. "Transonic and low-supersonic aero elastic analysis of a two-degree-of-freedom airfoil with a freeplay non-linearity", *Journal of Sound and Vibration*. 234. 859-880. 2000.
16. Davinder Rana, Sandeep Patel, A. K. Onkar and M. Manjuprasad, "Time domain simulation of airfoil flutter using fluid structure coupling through FEM based CFD solver", *Inproceedings, Symposium on Applied Aerodynamics and Design of Aerospace Vehicle*, 2011.
17. N. Razak, T. Andrianne, G. Dimitriadis, Bifurcation analysis of a wing undergoing stall flutter oscillations in a wind tunnel, 2013.
18. C. De Marqui Jr, D. Rebolho, E. Belo, F. Marques, R. Tsunaki, Design of an experimental flutter mount system, *Journal of The Brazilian Society of Mechanical Sciences and Engineering - J BRAZ SOC MECH SCI ENG*, 29, 10.1590/S1678-58782007000300003, 2007.
19. D. Tang, E. H. Dowell, Computational/Experimental Aero elastic Study for a Horizontal-Tail Model with Free Play, *AIAA Journal*, 51, pp. 341-352, 10.2514/1.J051781, 2013.
20. M. I. Babar, A. Javed, F. Mazhar, R. Latif, Experimental Flutter analysis of the Wing in Pitch and Plunge Mode, *Sixth International Conference on Aerospace Science and Engineering (ICASE)*, pp. 1-7, 10.1109/ICASE48783.2019.9059148, 2019.
21. N. Razak, T. Andrianne, G. Dimitriadis, Flutter and Stall Flutter of a Rectangular Wing in a Wind Tunnel, *AIAA Journal*, 49, pp. 2258-2271, 10.2514/1.J051041, 2011.
22. R. S. Vihar, J. V. M. L. Jeyan, K. S. Priyanka, Effect of camber on the flutter characteristics of different selected airfoils, *INCAS BULLETIN*, (print) ISSN 2066–8201, (online) ISSN 2247–4528, ISSN–L 2066–8201, vol 13, issue 3, pp. 215-223, <https://doi.org/10.13111/2066-8201.2021.13.3.18>, 2021.
23. D. Hodges, G. Pierce, and M. Cutchins, Authorized licensed use limited to: Auckland University of Technology. *Introduction to Structural Dynamics and Aeroelasticity*, vol. 56, no. 3. 2003.
24. R. H. Scanlan, F. Sisto, E. H. Dowell, H. C. Curtiss, and H. Saunders, *A Modern Course in Aeroelasticity*, vol. 103, no. 2. 2010.

25. R. M. Bennett, "Test Cases for Flutter of the Benchmark Models Rectangular Wings on the Pitch and Plunge Apparatus," 2002.
26. Bernard Etkin. Turbulent Wind and Its Effect on Flight. *Journal of Aircraft*, 18(5):327_345, 1981. doi:10.2514/3.57498.
27. Liu, J., and Chan, H., "Limit Cycle Oscillations of Wing Section with Tip Mass," *Nonlinear Dynamics*, Vol. 23, No. 3, 2000, pp. 259–270. doi:10.1023/A:1008361430662
28. Gomez, J. C., and Garcia, E., "Morphing Unmanned Aerial Vehicles," *Smart Materials and Structures*, Vol. 20, No. 10, 2011, Paper 103001. doi:10.1088/0964-1726/20/10/103001
29. Xu, J., and Ma, X. P., "Effects of Parameters on Flutter of Wing with an External Store," *Advanced Materials Research*, Vol. 853, 2014, pp. 453–459, <https://www.scientific.net/AMR.853.453>.
30. Livne, E, "Aircraft Active Flutter Suppression: State of the Art and Technology Maturation Needs", *Journal of Aircraft*, Vol. 55, No. 1, Jan.-Feb. 2018, pp. 410-452, doi: 10.2514/1.C034442.
31. Theodorsen, Th.: *General Theory of Aerodynamic Instability and the Mechanism of Flutter*. NACA Rept.496 (1934)
32. L. Marchetti, A. De Gaspari, L. Riccobene, F. Toffol, F. Fonte, S. Ricci and P. Mantegazza, *Active Flutter Suppression Analysis and Wind Tunnel Studies of an Uncertain Commercial Transport Configuration*,(2022), doi: 10.2514/6.2020-1677
33. Ivo Miguel Delgado Rocha, *Experimental and Numerical Aeroelastic Study of Wings*, 2019

2) APPENDIX

Code:

Here is the code that is used to detect the acceleration data variations that occurred in the test section of the wind tunnel. This code is executed in **arduino 1.8.19 software**

```
#include <Wire.h>

// Wire library - used for I2C communication
int ADXL345_a = 0x53;
// The ADXL345 sensor I2C address
// SDO-> Vcc
// SDO-> GND
float Xa_out, Ya_out, Za_out;
// Outputs from Acce A

void setup()
{
  Serial.begin(9600);
  // Initiate serial communication for printing the results on the Serial monitor
  Wire.begin();
  // Initiate the Wire library
  // Set ADXL345 in measuring mode
  Wire.beginTransmission(ADXL345_a);
  // Start communicating with the device
  Wire.write(0x2D);
  // Access/ talk to POWER_CTL Register - 0x2D
  // Enable measurement
  Wire.write(8);
  // (8dec -> 0000 1000 binary) Bit D3 High for measuring enable
  Wire.endTransmission();
  delay(10);
}

void loop()
{
  // === Read accelerometer data from a === //
  Wire.beginTransmission(ADXL345_a);
  Wire.write(0x32);
  // Start with register 0x32 (ACCEL_XOUT_H)
  Wire.endTransmission(false);
  Wire.requestFrom(ADXL345_a, 6, true);
  // Read 6 registers total, each axis value is stored in 2 registers
  Xa_out = ( Wire.read() | Wire.read() << 8);
  // X-axis value
```

```

Xa_out = Xa_out/256;
    //For a range of +-2g, we need to divide the raw values by 256, according to the
    // datasheet
Ya_out = ( Wire.read()| Wire.read() << 8);
    // Y-axis value
Ya_out = Ya_out/256;
Za_out = ( Wire.read()| Wire.read() << 8);
    // Z-axis value
Za_out = Za_out/256;

Serial.print("Xa= ");
Serial.print(Xa_out);
Serial.print(" Ya= ");
Serial.print(Ya_out);
Serial.print(" Za= ");
Serial.println(Za_out);

}

```

Here is the brief on the **MATLAB code** we used in this experimental process of obtaining different plots.

```

clc
clear
close all
    %% READING ACCELEROMETER DATA and defining Variables
    %% LEADING EDGE %%
data = xlsread('LE_500rpm.csv');
    % Importing accelerometer data
LE_time = data(:,1);
    % Assigning variables - time
LE_X_acc = data(:,2)
    % Assigning variables - X acceleration
LE_Y_acc = data(:,3);
    % Assigning variables - Y acceleration
LE_Z_acc = data(:,4);
    % Assigning variables - Z acceleration
    %% FFT %%
N = numel(LE_time);
    % Number of time steps
Ts = abs(diff(LE_time(1:2)));
    % time interval per time step which is sampling time period
fs = 1/Ts;
    % Converting sampling time period to sampling frequency

```

```

f_axis = [0:N-1]*fs/N;
           % fs returns number of interval not frequency value, so here we
convert fs to frequency value using DFT(Discrete Fourier Transform) relations
A_freq_LE = fft(LE_Z_acc);
           % Converting acceleration values from time domain to frequency
domain using fast fourier transform

figure(1)
hold on
           % hold on is used to plot multiple curves in same graph
plot(f_axis,abs(A_freq_LE),'-r','LineWidth',0.5)
           % plotting frequency vs acceleration graph for LE

grid on
grid minor
           % TRAILING EDGE %
data = xlsread('TE_500rpm.csv');
           % Importing accelerometer data
TE_time = data(:,1);
           % Assigning variables - time
TE_X_acc = data(:,2);
           % Assigning variables - X acceleration
TE_Y_acc = data(:,3);
           % Assigning variables - Y acceleration
TE_Z_acc = data(:,4)
           % Assigning variables - Z acceleration

           %% FFT %%

N = numel(TE_time);

Ts = abs(diff(TE_time(1:2)));
           % Number of time steps
           % time interval per time step which is sampling time period

fs = 1/Ts;
           % Converting sampling time period to sampling frequency
f_axis = [0:N-1]*fs/N;
A_freq_TE = fft(TE_Z_acc);
           % fs returns number of interval not frequency value, so here we
convert fs to frequency value using DFT(Discrete Fourier Transform) relations
           % Converting acceleration values from time domain to frequency
domain using fast fourier transform
figure(1)

plot(f_axis,abs(A_freq_TE),'-b','LineWidth',0.5)
           % plotting frequency vs acceleration graph for TE

grid on
grid minor

```

```
ylabel('Acceleration amplitude (m/s^2)','FontSize',14,'FontWeight','normal')
    % Giving axis labels
xlabel('Frequency (Hz)','FontSize',14,'FontWeight','normal')
    % Giving axis labels
ylim([0 20])
    % Giving limit values for Y axis
legend ('Leading Edge','Trailing Edge','FontSize',12,'FontWeight','normal')
    % Assigning legend to plot for LE and TE curves
title('Acceleration vs Frequency - NACA 24015 at 0 \circ
AOA','FontSize',16,'FontWeight','normal')
    % Giving title to graph
```

3) LIST OF PUBLICATIONS:

1. Vihar, Rampalli & Jeyan, Dr & Priyanka, K.. (2022). Experimental Study of Flutter Characteristics of Selected Wing Plan forms for the Effect of Camber. INCAS BULLETIN. 14. 133-144. 10.13111/2066-8201.2022.14.3.12.
2. Vihar, Rampalli & Jeyan, Dr & Priyanka, K.. (2021). Effect of camber on the flutter characteristics of different selected airfoils. INCAS BULLETIN. 13. 215-223. 10.13111/2066-8201.2021.13.3.18.
3. Jeyan, Dr & Vihar, Rampalli & Priyanka, K.. (2021). Design and analysis for the flutter behavior of different selected wing plan forms computationally. IEEE Access. 72-78. 10.1109/ICPS51508.2020.00018.
4. Jeyan, Dr & Vihar, Rampalli & Priyanka, K.. (2020). A Review on Aerodynamic Parameters, Methodologies and Suppression Techniques Explored in Aircraft Wing Flutter. International Journal of Nanomechanics Science and Technology. 29. 3494-3505.